collected in Table 2 show the expected pattern. For the fully optimized cluster C, there is close agreement between 6-31G(d) and 6-31G(d,p) results: bond lengths differ by about 0.004 Å for the O-H bond, Si-O and Al-O bonds are virtually equal and Si-O-H bond angles vary by 0.3°. Comparing the fully optimized cluster C with its partially optimized structure, the Al-O bonds of the latter are longer while the Si-O bonds are slightly shorter than the former. The 6-31G(d,p) calculations of the partially optimized structure yields an O-H that is 0.002 Å too short. The comparative results for the optimized 'cluster C' (Si/Al = 4) and optimized 'cluster B' having high silica zeolite (Si/Al = 10) demonstrate the variation of acidity on chemical composition of Si/Al ratio i.e the acid strength of zeolite increases with decreasing Al content, which is in accordance with recent experimental data [41].

3.2. Proton affinities

Proton affinities (PAs) of Brønsted hydroxyl group in zeolites are considered to be an important feature of catalytic activity. The performance of the B3LYP method in predicting gas phase proton affinities is compared with highly the reliable coupled pair functional method [35] and G1 theory [42,43]. Both theoretical levels are reportedly capable of predicting PAs accurate to within 2 to 3 kcal/mol. All calculated PAs at different basis sets for different cluster models are documented in Table 3.

3.2.1. Silanol

The B3LYP/6-311G(d,p) and B3LYP/6-311 + G(d,p) proton affinites are found to be 368.6 and 363.7 kcal/mol. It is clearly seen that inclusion into the basis of a single diffuse function on heavy atoms,

Table 3

OH bond lengths (Å), proton affinities (PA in kcal/mol) and Mulliken charges of the acidic hydrogens computed with the B3LYP for the different models

Model	Basis set	[₹] OH	PA	q_{H}	
H ₂ O	6-31G(d)	0.969	431.8	0.3871	
•	6-31G(d,p)	0.965	435.1	0.3049	
	6-311G(d)	0.962	425.4	0.3987	
	6-311G(d.p)	0.962	429.2	0.2367	
	6-311 + G(d,p)	0.962	396.0	0.2529	
Н ₃ СОН	6-311G(d)	0.963	397.2	0.3789	
•	6-311G(d,p)	0.961	401.2	0.2355	
H ₃ SiOH	6-311G(d,p)	0.959	368.8	0.2808	
•	6-311 + G(d,p)	0.959	363.7	0.2814	
H ₃ AIOHSiH ₃	6-311G(d,p)	0.963	314.3	0.3427	
•	6-311 + G(d,p)	0.963	312.6	0.3303	
Cluster C ^a	6-31G(d)	0.971	306.7	0.4768	
	6-31G(d,p)	0.968	310.5	0.3777	
	6-311G(d)	0.964	304.4	0.4882	
	6-311G(d,p)	0.964	307.5	0.3568	
Cluster C b	6-31G(d)	0.974	303.6	0.4740	
Cluster B *	6-31G(d)	0.972	300.9	0.4773	
	6-311G(d,p)	0.965	301.9	0.3497	
H ₃ O ⁺	6-31G(d)	0.982	173.8	0.5576	
-	6-31G(d,p)	0.976	178.2	0.4653	
	6-311G(d)	0.973	176.1	0.5796	
	6-311G(d,p)	0.975	176.1	0.4193	
	6-311 + G(d,p)	0.976	170.0	0.4182	

Partially optimized structure.

b Fully optimized structure.

 $6-311G(d,p) \rightarrow 6-311 + G(d,p)$, yields a significant improvement in the PA. The DFT performs perfectly well at the B3LYP/6-311 + G(d,p) level, which is in good agreement with the CPF and G1 results (363.5 and 363.4 kcal/mol).

3.2.2. Zeolites

A nearly linear relationship between the PAs and the net charge on the proton, q_H , has been derived for a set of structurally related molecules (HO-H, H₃CO-H, H₃SiO-H, H₃SiOHAlH₃, different types of zeolite cluster models, and H₃O⁺) and is illustrated in Fig. 2. As expected, the hydronium cation yields the lowest PA, while the nonacidic water molecule provide the largest PA value. Comparing the PAs of H, SiOH with H, SiO(H)AlH, the PA of the latter is 50.9 kcal/mol lower than the PA of the former which corresponds to the lengthening of the OH in the H₃SiO(H)AlH₃. This results from the interaction of the Lewis acid, AlH3, with the basic oxygen site in the Lewis acid-base complex, $H_3SiOH...AlH_3$. The B3LYP/6-311G+(d,p) result of the PA for [H3SiOAlH3] is also encouraging. The deviation from the most accurate G1 [38,39] is about 2.86 kcal/mol. The MP2/DZ2P proton affinity yields a virtually identical value to the less expensive B3LYP result (312.5 kcal/mol (MP2) versus 312.6 kcal/mol (B3LYP)).

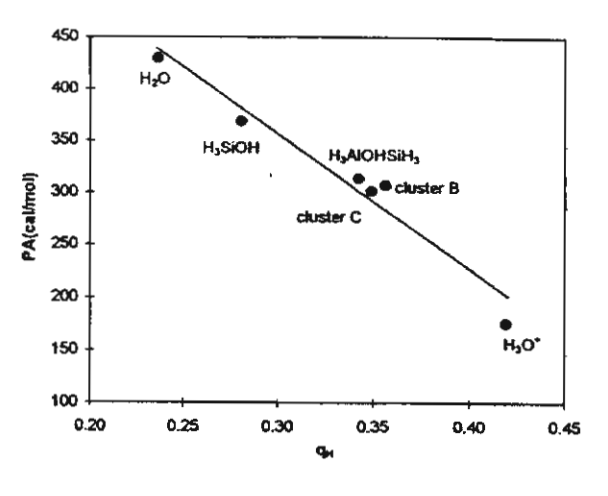
For cluster C, $Al(OSiH_3)_4H$, the B3LYP/6-311G(d,p) calculation yields a PA value of 307.5 kcal/mol. It is also important to study the dependence of PA on the employed cluster size. On expanding the model cluster from $H_3SiO(H)AlH_3$ to $Al(OSiH_3)_4H$, PA is decreased by 6.8 kcal/mol. For the largest faujasitic zeolite model, Fig. 1b, the PA is evaluated to be 301.9 kcal/mol. Using the systematic deviation between B3LYP/6-311G+(d,p) and G1 theory, our predicted value is estimated to be 294 ± 3 kcal/mol, which is in the range of experimentally determined values of 291-300 kcal/mol [44,45].

3.3. The interaction of faujasitic zeolite with water

3.3.1. Structures and energetics

Two representative cluster models of water adsorption on zeolites are investigated. In one of these, the hydrogen-bonded structures are stabilized on the

B3LYP/6-311G(d,p)



B3LYP/6-311+G(d,p)

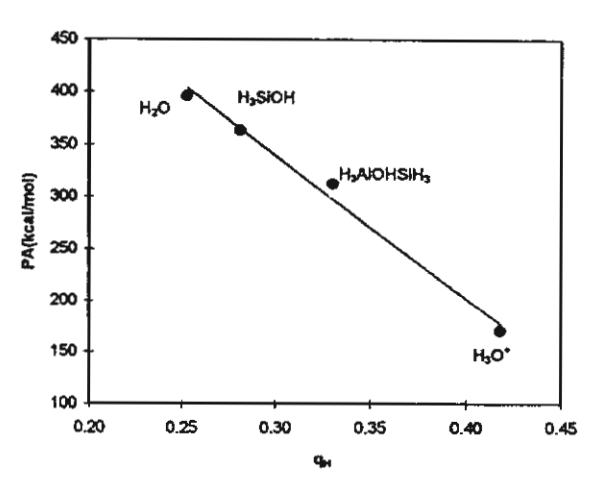


Fig. 2. The proton affinities of a set of structurally related molecules (HO-H, H_3 COH, H_3 SiO-H, H_3 SiOHAl H_3 , different types of zeolite cluster models, and H_3 O⁺) as a function of the net charge on the proton, q_H .

bridging OH. The other is a type of protonated model, in which hydronium cation forms two hydrogen bonds towards the unprotonated zeolitic framwork. Attempts were made to search for the minimum structure of zeolite cluster model/H₃O⁺. All investigated cluster models yield only one minimum as hydrogen-bonded physisorbed water complexes regardless of whether the initial framework structure having H₂O or hydronium ion. It is noted that in the case of ion-pair complexes, an initial structure with a

J. Limirakul ei al. / Chemical Physics 215 (1997) 77-87

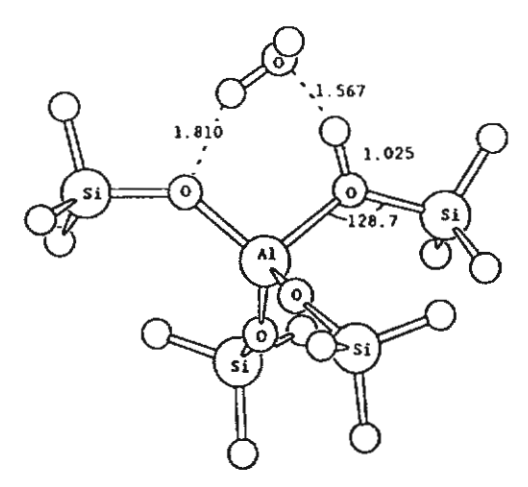


Fig. 3. Schematic representation of molecular model for the cluster C, Al(OSiH₃)₄H/H₂O.

hydronium ion is optimized. The OH bond of H₃O⁺ and the hydrogen bond angle (O...H-O) in the complex is constrained at the optimized H₃O⁺ and 180, respectively. The final complex can be derived by removing the fixed internal coordinates from the former constrained optimization structure. Similar conclusions to our predicted results have just recently been reported by Sauer et al. [11]. Recent FT-IR [17] and ab initio [14] studies of H₂O adsorption on zeolite support the direct clear evidence for the hydrogen-bonded adsorption of water. In the present study we concentrate only on the most probable hydrogen-bonded models.

The optimized geometry of cluster C with water (Fig. 3) and the extended model cluster B with water (Fig. 4) are investigated at the B3LYP/6-31G(d) level. The geometric parameters are summarized in Table 4. The results for the surface complexes clus-

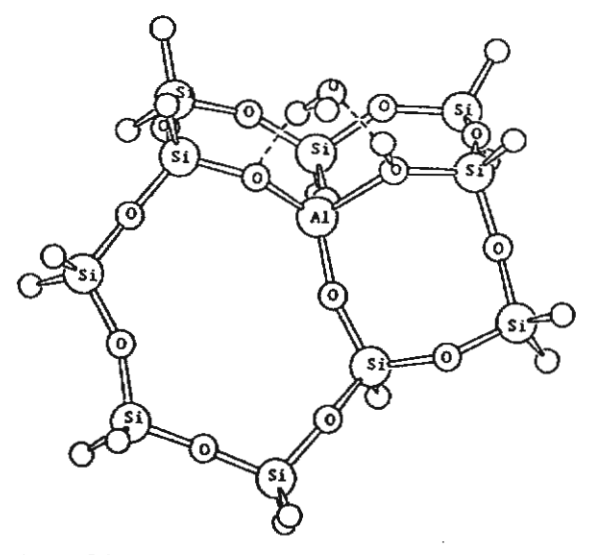


Fig. 4. Schematic representation of molecular model for the faujasitic zeolite/water.

ter C/water and cluster B/water indicate that the adsorbed water can act both as a proton acceptor and as a proton donor. The two hydrogen bonds are part of a cyclic structure, which have also been reported at HF/DZP level of theory by Sauer et al. [13].

The changes in the structural parameters of the faujasitic zeolite upon complexation with water are impressive. The results are in accordance with Gutmann's rules [46], i.e. a lengthening of the bridging O-H bond, a shortening of Al-O adjacent to this bond and a lengthening of Al-O (not adjacent to it).

The intermolecular O...O distance in the optimized and rigid structure of faujasite/water adducts (within the O-H...O hydrogen bond) are evaluated to be 2.605 and 2.555 Å, respectively. The con-

Table 4
B3LYP optimized structure parameters for Al(OSiH₃)₄H/H₂O (cluster C, cf. Fig. 3) and faujasitic zeolite catalyst/water (cluster B, cf. Fig. 4)

Model/parameter	Rigid cluster C	Optimized cluster C	Rigid cluster B	Optimized cluster B
r _{AlO}	1.961	1.912	1.953	1.909
rsio	1.729	1.714	1.726	1.710
r _{OH}	0.964	1.026	0.965	1.024
^г о(н)о	2.598	2.546	2.605	2.555
r _н о	1.685	1.567	1.693	1.581
r _{он}	1.933	1.811	1.981	1.863
∠ _{Al-O-Si}	128.0	128.8	128.7	129.2

tracted O...O distance of the latter model reflects an increase of the binding energy (-20.3 versus -22.5 kcal/mol). The adsorption energy for the largest model investigated, cluster B (Fig. 1b) is -20.3 kcal/mol, which is close to the result for the smaller cluster C (-20.5 kcal/mol, Fig. 1c). The binding energy of the latter cluster can be compared to the MP2 result of Sauer et al. [11] (-20.3 versus -18.98 kcal/mol). The heat of adsorption of water with H-ZSM-5 has been recently obtained by Gorte [[15],[16]], which is an excellent agreement with our largest model (-20.4 versus -20.3 kcal/mol).

In order to check the reliability of the calculated intermolecular O...O distance of faujasite/water, the water dimer was also carried out and compared to the experimental data. The calculated O...O distance of water dimer is found to be 2.909 Å, only 0.009 Å longer than the corresponding MP2 value and 0.03 Å less than the experimentally determined value of the O...O distance [47].

In order to compare the relative acidity with the other types of hydrogen-bonded systems we have performed calculations with the same theoretical model on the systems $HF...H_2O(-11.68)$, $HCl...H_2O(-8.94)$, $H_3SiOH...H_2O(-9.52)$ and $H_3SiOHAlH_3...H_2O$ (-19.24); the values in parentheses are the hydrogen bonding energies in kcal/mol. The B3LYP results suggest that in comparison with hydrogen halides, the faujasitic zeolite/ H_2O system is a strong acid.

3.3.2. Analytical potentials

The interaction of faujasite catalyst with water for different conformations has been calculated at DFT and HF levels of theory. The Hartree-Fock calculations were performed with the effective-core potential and corresponding basis sets of Stevens et al. [48-50] (denoted as SBKJC) in valence doule-zeta contraction. For the DFT calculations the B3LYP functional and the 6-31G(d) basis set were used. In order to construct potential functions for faujasitic zeolite/water, four main steps have been employed: (1) selection of the dimer conformations, (2) perfoming the B3LYP/6-31G(d) and HF/SBKJC calculations, (3) selecting the analytical form, and (4) fitting the computed DFT/B3LYP and HF/SBKJC energies to the selected functional forms.

The water geometry has been kept at the experimental values ($r_{OH} = 0.9572 \text{ Å}$, $\angle HOH = 104.52^{\circ}$ [51]), while the faujasite structure has been taken from the B3LYP/6-311G(d,p) optimization. Fig. 5 shows the faujasitic zeolite/water potential curves as a function of the O...H distance for three different levels of theory. The figure also reveals that HF/STO-3G yields a steeper minimum at a shorter distance than B3LYP/6-31G(d). This large difference shows that calculations on the STO-3G level are not useful here. The HF/SBKJC results are encouraging when compared to B3LYP/6-31G(d). The two potential curves are quite similar despite of the fact that the HF/SBKJC calculations are much

Table 5
Atomic charges for water and faujasite (cluster B)

Water molecule					
O = -0.7401					
H = 0.3700					
Faujasite (Cluster B)					
H1 = -0.1356	H10 = -0.1445	H14 = -0.1465	H15 = -0.1449	H16 = -0.1365	,
H21 = 0.5165	H23 = -0.1490	H24 = -0.1663	H28 = -0.1197	H33 = -0.1630	
H34 = -0.1621	H35 = -0.1613	H36 = -0.1313	H38 = -0.1551	H39 = -0.1428	
H41 = -0.1650	H42 = -0.1639	O3 = -1.1567	O4 = -1.0252	O5 = -1.0110	
O9 = -1.1400	O11 = -1.1141	O12 = -1.0356	O13 = -1.0424	O17 = -1.0340	
O22 = -1.0249	025 = -1.0048	Q26 = -1.0156	O27 = -1.0398	O32 = -1.0168	
O37 = -1.0271	A16 = 1.9752	Si2 = 1.5934	Si7 = 1.3417	Si8 = 1.3511	
Si18 = 1.6386	Si19 = 1.6427	Si20 = 1.6616	Si29 = 1.3454	Si30 = 1.3438	
Si31 = 1.3254	Si40 = 1.3404				

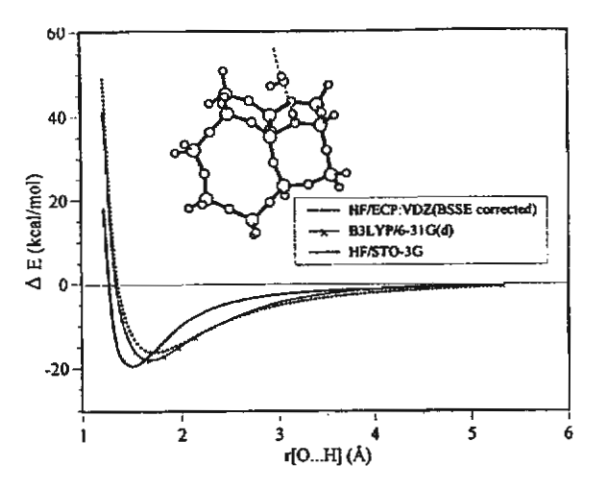


Fig. 5. Comparison of adsorption energies from B3LYP/6-31G(d), HF/ECP-VDZ, and HF/STO-3G for the faujasitic zeolite/water system.

faster (on an SGI Challenge about 50 times). After testing a variety of functional forms, a simple 2-6-10-12 potential energy expression for the interaction of faujasitic zeolite with water was employed:

$$E_{\text{fit}}^{z-w}(r_{ki}) = \sum_{k,i} \left[\frac{q_k q_i}{r_{ki}} + \frac{A_{ki}}{r_{ki}^2} + \frac{B_{ki}}{r_{ki}^6} + \frac{C_{ki}}{r_{ki}^{10}} + \frac{D_{ki}}{r_{ki}^{12}} \right].$$

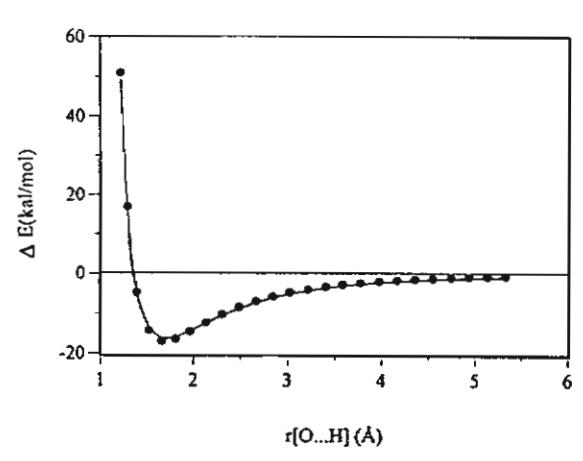


Fig. 6. Comparison between ab initio energy surface data (Δ) and analytical potential curves (lines) for the configuration presented in Fig. 4.

 r_{ki} is the distance between atom k on the zeolite molecule and atom i on the water molecule. q_k and q_i are atomic charges taken from a Mulliken population analysis (cf. Table 5). A_{ki} , B_{ki} , C_{ki} and D_{ki} are the parameters determined by least-squares fitting. The fitted parameters of the potential energy functions are tabulated in Table 6 (in kcal/mol). The quality of the fit is illustrated in Figs. 6 and 7. Fig. 6

Table 6
The fitted parameters of the potential energy functions (see text)

Parameter	A	В	С	D
H1-O	-1.0331905×10^{2}	1.8382883 × 10 ²	-1.5083348×10^{2}	8.9420565 × 10 ¹
H1-H	1.2645426×10^{2}	-2.8999846×10^{2}	2.4324152×10^{2}	-5.5234880×10^{2}
H2-O	2.8574043×10^{1}	5.2740608×10^{2}	-3.3482893×10^{2}	-2.6299890×10^{2}
H2-H	-8.3599299×10^{1}	1.4191032×10^{2}	5.9935692×10^{1}	-1.0575208×10^{2}
01-0	-2.2914121×10^{1}	1.3536682×10^{3}	-3.9274513×10^{3}	6.0327825×10^{3}
O1-H	-9.2895111×10^{1}	1.2641836×10^{2}	-3.6371045×10^{1}	1.2479447×10^{1}
O2-O	2.5865495×10^{2}	-1.3296107×10^{3}	1.5674254×10^{5}	-3.4876443×10^{5}
O2-H	-1.1555464×10^{2}	2.1024226×10^{2}	-1.9198437×10^{2}	1.0763633×10^{2}
O3-O	2.8803433×10^{2}	-6.7006798×10^{2}	1.0924449×10^{5}	-2.4821535×10^{5}
O3-H	-1.4723644×10^{2}	1.9241469×10^{2}	6.6505733×10^{2}	-1.0651945×10^{3}
04-0	-7.4289775×10^{1}	1.9661823×10^{3}	4.0700384×10^{3}	-1.2381189×10^4
O4-H	-1.3862499×10^{2}	4.6499706×10^{1}	7.3627116×10^{3}	1.8873061×10^{3}
O5-O	-3.2716430×10^{0}	8.9273658 × 101	2.8112535×10^{5}	-1.1607496×10^6
O5H	-1.1941986×10^{2}	1.4535989×10^{2}	2.1379764×10^{3}	-3.3723297×10^{3}
O6-O	-1.1715990×10^{2}	1.5436984×10^{3}	2.0774143×10^4	-8.0412282×10^4
O6-H	-9.7118742×10^{1}	1.7816578×10^{2}	-1.3496463×10^{2}	7.1361063×10^{1}
Si1-O	-5.7071178×10^{1}	-2.3134268×10^{3}	8.2071595×10^4	-4.9494428×10^4
Sil-H	2.8669836×10^{2}	-2.9201129×10^{2}	3.0196516×10^{3}	-3.7259970×10^{3}
Si2-O	1.6333832×10^{2}	-4.9009698×10^{0}	3.4294755×10^{5}	-1.4582774×10^{5}
Si2-H	2.3662032×10^{2}	$-1.2223283 \times 10^{\circ}$	2.2845654×10^4	-5.9072913×10^4
Al-O	-5.1438777×10^{2}	1.1459039×10^{3}	1.3088621×10^{5}	-5.1532513×10^{5}
Al-H	1.1556943×10^{2}	5.7061768×10^{2}	-9.1190710×10^{3}	1.4812055×10^4

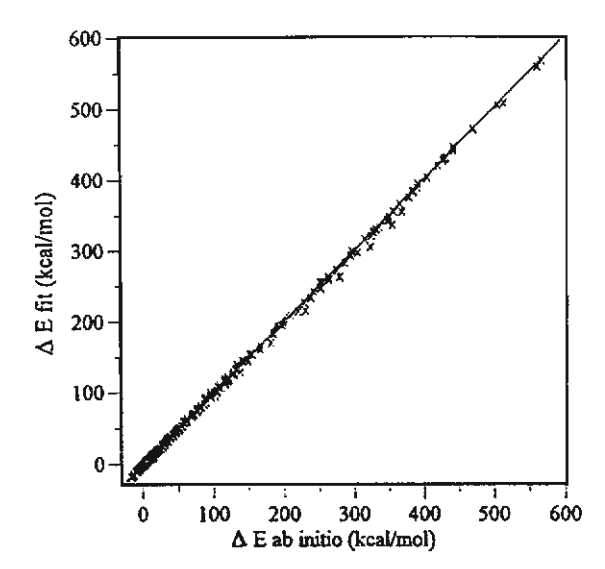


Fig. 7. Correlation between interaction energy ($\Delta E_{ab~laitio}$) from the ab initio calculations and those derived from analytical expressions as described in the text.

shows the fitted values for the same curve as Fig. 5 whereas Fig. 7 illustrates the correlation between all ab initio and fitted energies. The standard deviation obtained between fitted and ab-initio energies is 2.14 kcal/mol. Since among the 500 points used in the fitting there are many with high energies, this is a good value. Our newly developed potentials will be further employed in the simulation of zeolite/water system.

4. Conclusions

We have presented a density-functional study of faujasitic zeolites and their complexes with water using the B3LYP functionals and the basis sets 6-31G(d), 6-31G(d,p), 6-311G(d), 6-311G(d,p) and 6-311 + G(d,p). The agreement between DFT/B3LYP-6-311 + G(d,p) proton affinities and the corresponding CPF and G1 values are excellent. Comparing the older BLYP and VWN functionals with the recently introduced B3LYP functionals, the latter yields superior accuracy. This artificial significant lengthening effect on the weaker Al-O bond in the BLYP and VWN calculations does not occur with B3LYP. The Si-O(H)-Al and Si-O-H bond angles of zeolites do not appreciably depend on the

inclusion of non-local effects in the density functional. The 6-31G(d) basis set in the DFT prediction of the faujasite structure yields good results and is an economic choice for large systems. The predicted PA of the faujasitic catalyst is estimated to be 294 ± 3 kcal/mol, which is in the range of experimentally determined value of 291-300 kcal/mol. The faujasite catalyst/water structure (see Fig. 1b) is stabilized at the bridging O-H group by two H-bonds with binding energy of -20.3 kcal/mol. Comparison with hydrogen halides and related complexes of water demonstrates that the faujasite is a strong acid. An analytical potential for the interaction fo faujasitic zeolite with water was derived by fitting the ab initio interaction energies which we plan to employ simulations studies of petrochemical catalyst/water systems.

Acknowledgements

This work was supported by donors of the Thai- I land Research Fund (TRF) and the Kasetsart University Research and Development Institute (KURDI) and by Jubiläumsfonds der Österreichischen Nationalbank (project 5621). Our sincere thanks are due to Professor R. Ahlrichs (Karlsruhe, Germany) for his continued support of this work. We would like to express our gratitude to the referees for their critical and useful remarks and suggestions on this paper.

References

- [1] J. Klinowski, Chem. Rev. 91 (1991) 1459.
- [2] J.M. Thomas, Sci. Am. 266 (1992) 82.
- [3] G.J. Kramer, R.A. Van Santen, C.A. Emeis and A.K. Nowak, Nature 363 (1993) 529.
- [4] E. Kassab, J. Fouquet, M. Allavena and E.M. Evleth, J. Phys. Chem. 97 (1993) 9034.
- [5] C.T.W. Chu and C.D. Chang, J. Phys. Chem. 89 (1985) 1569.
- [6] K.J. Chao and L.J. Leu, Zeolite 9, (1989) 193.
- [7] J. Das, C.V.V. Satyanaryana, D.K. Chakrabarty, S.N. Pira-manayagarn and S.N. Shringi, J. Chem. Soc. Faraday Trans. 88 (1992) 3255.
- [8] Y. Murakami, A. Iijima and J.W. Ward, New Developments in Zeolite Science and Technology (Kodansha, Tokyo, 1986).
- [9] E. Nusterer, P.E. Blöchl and K. Schwarz, Chem. Phys. Lett. 253 (1996) 448.

- [10] S.A. Zygmunt, L.A. Curtiss, L.E. Iton and M.K. Erhardt, J. Phys. Chem. 100 (1996) 6663.
- [11] M. Krossner and J. Sauer, J. Phys. Chem. 100 (1996) 6199.
- [12] J. Sauer, P. Vglieugo, E. Garrone and V.R. Saunders, Chem. Rev. 94 (1994) 2095.
- [13] J. Sauer, H. Horn, M. Häser and R. Ahlrichs, Chem. Phys. Lett. 26 (1990) 173.
- [14] F. Haase and J. Sauer, J. Am. Chem. Soc. 117 (1995) 3780.
- [15] A. Ison and R.J. Gorte, J. Catal. 89 (1984) 150
- [16] R.J. Gorte, 1993, personal communication as referred by ref. 11
- [17] F. Wakabayashi, J.N. Kondo, K. Domen and C. Hirose, J. Phys. Chem. 100 (1996) 1442.
- [18] J. Limtrakul, J. Yoinuan, Chem. Phys. 184 (1994) 51; J. Limtrakul, Chem. Phys. 193 (1995) 79; J. Limtrakul and D. Tantanak, J. Mol. Struct. 358 (1995) 179; J. Limtrakul and D. Tantanak, Chem. Phys. 208 (1996) 331.
- [19] J.W. Andzelm and J.K. Labanowski, eds., Density Functional Methods in Chemistry (Springer, New York, 1991).
- [20] R.D. Amos, C.W. Murray, and N.C. Handy, Chem. Phys. Letter 202 (1993) 487.
- [21] N.C. Handy, P.E. Maslen, R.D. Amos, J.S. Andrew, C.W. Murray and G.I. Laming, Chem. Phys. Lett. 197 (1992) 506.
- [22] F. Sim, A. St-Amant, I. Papai and D.R. Salahub, J. Am. Chem. Soc. 114 (1992) 4391.
- [23] D.A. Dixon, J. Andzelm, G. Fitzgerald and E. Wimmer, J. Phys. Chem. 95 (1991) 9197.
- [24] J. Andzelm, E. Rodzio and D.R. Salahub, J. Comput. Chem. 6 (1985) 520.
- [25] P.J. Stephens, F.J. Devlin, L.F. Chablowski and M.J. Frisch, J. Phys. Chem. 98 (1994) 11623.
- [26] A.D. Becke, Phys. Rev. A 38 (1988) 3098; C. Lee, W. Yang and R.G. Parr, Phys. Rev. 13 (1988) 785.
- [27] C.W. Bauschlicher Jr. and H. Partridge, Chem. Phys. Lett. 240 (1995) 533-540.
- [28] J.W. Finley and P.J. Stephens, J. Mol. Struct (Theochem) 357 (1995) 255-235.
- [29] J. Limtrakul, unpublished results.
- [30] S.H. Vosko, L. Wilk and M. Nuisar, Can. J. Phys. 58 (1980) 1200.

- [31] M.J. Frisch, G.W. Trucks, H.B. Schlegel, P.M.W. Gill, B.G. Johnson, M.W. Wong, J.B. Foresman, M.A. Robb, M. Head-Gordon, E.S. Replogle, R. Gomperts, J.L. Andres, K. Raghavachari, I.S. Binkley, C. Gonzalez, R.L. Martin, D.J. Fox, D.J. DeFrees, J. Baker, J.J.P. Stewart and J.A. Pople, Gaussian 94 (Gaussian Inc., Pittsburgh, PA, 1994).
- [32] R. Ahlrichs, R. Baer, M. Haeser, H. Horn and C. Koemel, Chem. Phys. Lett. 162 (1989)165.
- [33] M. Haeser and R. Ahlrichs, J. Comput. Chem. 10 (1989) 104
- [34] J. Almloef, K. Faegri Jr. and K. Korsell, J. Comput. Chem. 3 (1982) 385.
- [35] J. Sauer and R. Ahlrichs, J. Chem. Phys. 93 (1990) 2575.
- [36] D. Freude, J. Klinowski and H. Hamdan, Chem. Phys. Lett. 149 (1988) 355.
- [37] A.K. Cheetham, M.M. Eddy and J.M. Thomas, J. Chem. Soc. Chem. Commun. (1988) 1337.
- [38] M. Eddy, PhD Thesis, University of Oxford, 1984.
- [39] J. Sauer, Chem. Rev. 89 (1989) 199.
- [40] J.J. Pluth and J.V. Smith, J. Am. Chem. Soc. 102 (1980) 4704.
- [41] D. Barthomeuf, Mater. Chem. Phys. 17 (1987) 49.
- [42] J.A. Pople, M. Head-Gordon, D. Fox, K. Raghavachari and L.A. Curtiss, J. Chem. Phys. 90 (1989) 5622.
- [43] L.A. Curtiss, C. Jones, G.W. Trucks, K. Raghavachari and J.A. Pople, J. Chem. Phys. 93 (1990) 2537.
- [44] J. Datka, M. Boczar and P. Rymarowicz, J. Catal. 114 (1988) 368
- [45] J. Datka, M. Boczar and B. Gil, Langmuir 9 (1993) 2496.
- [46] V. Gutmann, The donor-acceptor approach to molecular interactions (Plenum Press, New York, 1978).
- [47] J.A. Odutola and T.R. Dyke, J. Chem. Phys. 72 (1980) 5062.
- [48] W.J. Stevens, H. Basch and M. Krauss, J. Chem. Phys. 81 (1984) 6062.
- [49] W.J. Stevens, M. Krauss, H. Basch and P.G. Jasien, Can. J. Chem. 70 (1992) 612.
- [50] T.R. Cundari and W.J. Stevens, J. Chem. Phys. 98 (1993) 5555
- [51] W.S. Benedict, N. Gailar and E.K. Plyler, J. Chem. Phys. 24 (1956) 1139.

Reprinted from

Journal of MOLECULAR STRUCTURE

Journal of Molecular Structure 435 (1997) 181-192

Coadsorption of ammonia and methanol on H-zeolites and alkaline-exchanged zeolites

Jumras Limtrakul*, Usa Onthong

Laboratory for Computational and Applied Chemistry, Chemistry Department, Faculty of Science, Kasetsart University, Bangkok 10900, Thailand





Journal of MOLECULAR STRUCTURE

Journal of Molecular Structure 435 (1997) 181-192

Coadsorption of ammonia and methanol on H-zeolites and alkaline-exchanged zeolites

Jumras Limtrakul*, Usa Onthong

Laboratory for Computational and Applied Chemistry, Chemistry Department, Faculty of Science, Kasetsart University,
Bangkok 10900, Thailand

Received 17 February 1997; revised 10 April 1997; accepted 10 April 1997

Abstract

The interactions of methanol and ammonia on H-zeolites (H-Z) and alkaline-exchanged zeolites (Na-Z) have been investigated using Hartree-Fock (HF) and density functional theory (DFT) approaches. Full optimization of all clusters and their complexes has been optimized at B3LYP/6-31G* and HF/6-31G* theoretical levels. The reaction mechanism of coadsorption of methanol and ammonia on H-Z is that the ammonia is found to bound to the Brønsted acid site of H-Z, yielding ammonium cation, which in turn operates as an active site for methanol. The result of coadsorption processes indicates that the stronger base ammonia is preferentially bonded to the Brønsted acid sites of H-Z, while methanol is interacted with the Lewis acid of Na-Z. Our findings are in excellent agreement with very recently reported data (Kogelbauer, A., Grundling, G., Lercher, J.A., J. Phys. Chem. 100 (1996) 1852–1837). © 1997 Elsevier Science B.V.

Keywords: Quantum chemical calculations; Adsorption; Catalysis; Zeolites; Methanol-ammonia interaction

1. Introduction

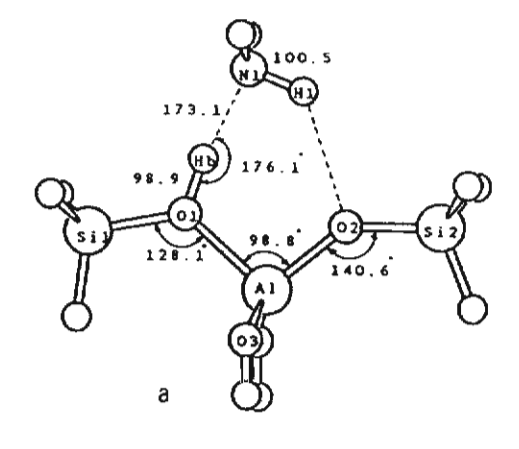
The acidity of zeolitic catalysts released from the surface hydroxyls (≡Si-OH-Al≡) is responsible for their catalytic function and has led to numerous important industrial applications, such as the application of catalysts and adsorbents in petrochemical processes and for the production of fine chemicals [1-15]. Of particular interest in this active research is the products generated from the adsorption of methanol (i.e. conversion of methanol to gasoline) [16-21] and the coadsorption of methanol and ammonia [22,23] (production of methylamines, which are essential chemical building subunits for important industrial materials such as resins, fibers,

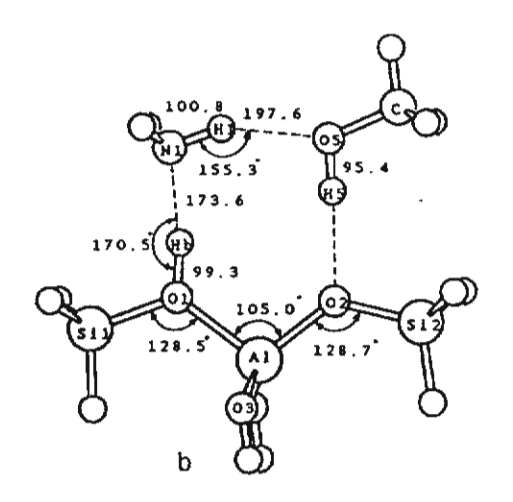
In this work, the interactions of methanol and ammonia with H-zeolites (H-Z) and alkaline-zeolites (Na-Z) are investigated for the first time by the density functional theory (DFT), and Hartree-Fock (HF) with the aim of; a) investigating the important consequences of different types of adsorbed probe molecules at low and high coverages, i.e. (CH₃OH)_n, (NH₃)_n, (CH₃OH)(NH₃) and (NH₃)(CH₃OH), where

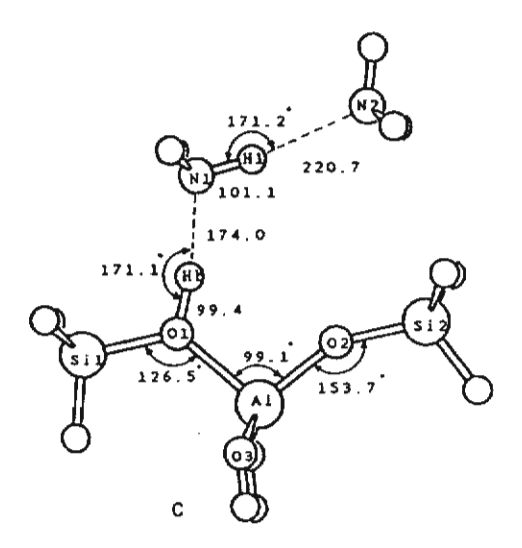
0022-2860/97/\$17.00 © 1997 Elsevier Science B.V. All rights reserved PII S0022-2860(97)00189-0

dyes and pharmaceuticals). One of the crucial steps of these chemically interesting systems involves the probed molecules adsorption on the catalyst surface. In spite of a large number of documents about zeolite research, details of the structures and reaction mechanisms of adsorption and, particularly of coadsorption, are still incomplete and only partially solved [17,23]. This understanding is the basis for the rational design of improved catalysts.

^{*} Corresponding author.







n denotes the amount of probed molecule coverages; b) determining the reaction mechanism of coadsorption; c) comparing the influence of H-Z and Na-Z on the coadsorption structure of methanol and ammmonia.

2. Method

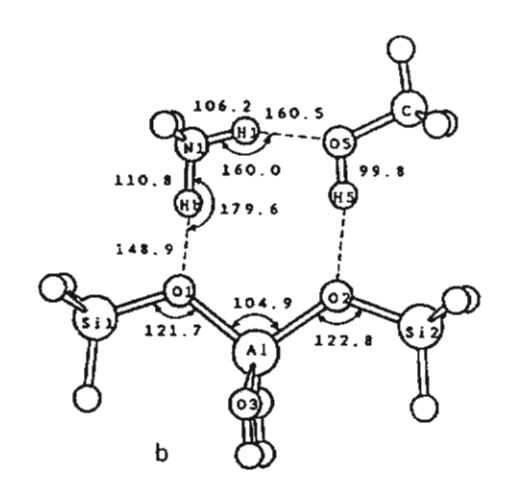
We employed the adsorption clusters illustrated in Figs. 1-3 as the models of the probed molecules' adsorption on zeolites {H₃SiOHAl(OH)₂OSiH₃}/ [NH₃][CH₃OH],and [H₃SiOHAl(OH)₂OSiH₃]/ [CH₃OH][NH₃], and their possible ion-pair species. The alkaline-exchanged systems, [H₃SiONaAl(OH)₂ OSiH₃]/[NH₃][CH₃OH] and [H₅SiONaAl(OH)₂ OSiH₃]/[CH₃OH][NH₃] are modelled for the coadsorption of methanol and ammonia on Na-exchanged zeolites (see Fig. 4 and Fig. 5). The isolated Nacomplexes, Na(I)/[NH₃][CH₃OH], and [CH₃OH][NH₃] are also included for comparison. We have also investigated the adsorption of methanol and ammonia at low and high coverages, with similar absorbent models of [H₃SiOHAl(OH)₂SiH₃]/ ICH₃OH₁. [H₃SiOHAl(OH)₂OSiH₃/[CH₃OH]₂, [H₃SiOHAl(OH)₂OSiH₃]/[NH₃], H₃SiOHAl(OH)₂ OSiH₃]/[NH₃]₂. In the models employed, the clusters have been terminated by hydrogen atoms.

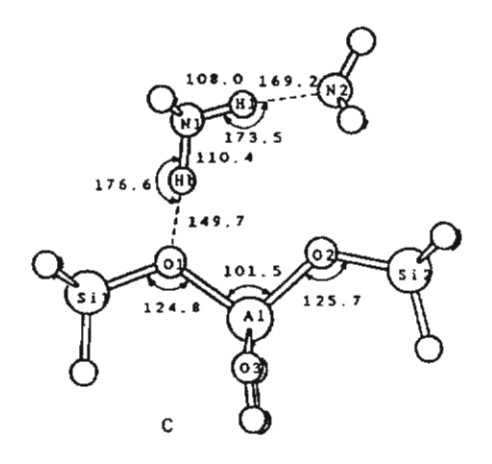
Full geometry optimization of the cluster models mentioned above was carried out with the DFT methods employing the B3LYP density functional. This functional has been recently demonstrated to yield accurate results for the molecular structures and vibrational frequencies for zeolites [24–26]. All density functional computations were performed using the program Gaussian-94 [27].

For the HF calculations, we employed the TURBO-MOLE code [28,29] which is based on the direct SCF method of Almloef et al. [30]. Geometry optimizations were terminated when the gradients norm with respect of internal coordinates was less than $10^{-3} E_b/a_0$. The energy change was then below 5×10^{-6} a.u.

The computations were carried out using DEC

Fig. 1. Schematic representation of molecular models for the systems Brønsted acid site [H₃SiOHAl(OH)₂OSiH₃]; (H-Z): a) [H₃SiOHAl(OH)₂OSiH₃]/[NH₃]; b) [H₃SiOHAl(OH)₂OSiH₃]/[NH₃].





Alphastation 250 and HP 9000/700 workstations at the Laboratory for Computational and Applied Chemistry at Kasetsart University.

3. Results and discussion

3.1. Coadsorption of ammonia and methanol on H-zeolite (H-Z)

3.1.1. Interaction of ammonia and methanol on H-Zeolite

The fully optimized geometrical structures constrained at Cs symmetry for [H₃SiOHAl(OH)₂OSiH₃]/[NH₃][CH₃OH] (see Fig. 1b) were investigated at HF levels of theory using 6-31G* basis set. The optimized parameters for the two theoretical approaches are summarized in Table 1.

Comparing the HF structure of H₃SiOHAl(OH)₂ OSiH₃ with the B3LYP structure, it is seen that the Si-O, Al-O and O-H bonds of the former are shorter than with the latter (see Table 2). Note that the HF results always yield an OH bond which is too short as compared to the experimental result [31].

Further support for the reliability of using this model is confirmed by the results of NMR measurement [32]: the Al...H of H-faujasite has been estimated to be $238 \pm 4 \,\mathrm{pm}$ whereas our computed distances at the B3LYP and HF levels of theory are 239.7 and 241.6 pm, respectively.

The changes in the structural parameters of tertiary upon complexation are in line with Gutmann's rules [33], i.e. a lengthening of the bridging OH bond, a shortening of Al-O and a lengthening of Al-O (not adjacent to the bridging OH bond).

In order to compare the structure and bonding with the related types of adsorbed molecules, we have also performed calculations on the systems H-Z/[NH₃], H-Z/[NH₃]₂. H-Z/[CH₃OH][NH₃], and H-Z/[CH₃OH] [CH₃OH] (see Table 4). The results suggest that the H-Z/[NH₃][CH₃OH] is energetically favoured in the coadsorption process of methanol and ammonia. The methanol has a pronounced effet on the H-Z/[NH₃] complex, indicating the capability of donating a

Fig. 2. Schematic representation of molecular models for the deprotonated framework {H₃SiOAl(OH)₂OSiH₃];(Z⁻): a) {H₃SiOAl(OH)₂SiH₃]⁻/{NH₄]⁺; b) {H₃SiOAl(OH)₂SiH₃]⁻/{NH₄]⁺(CH₃OH); c) {H₃SiOAl(OH)₂SiH₃]⁻/{NH₄]⁺(NH₃}.

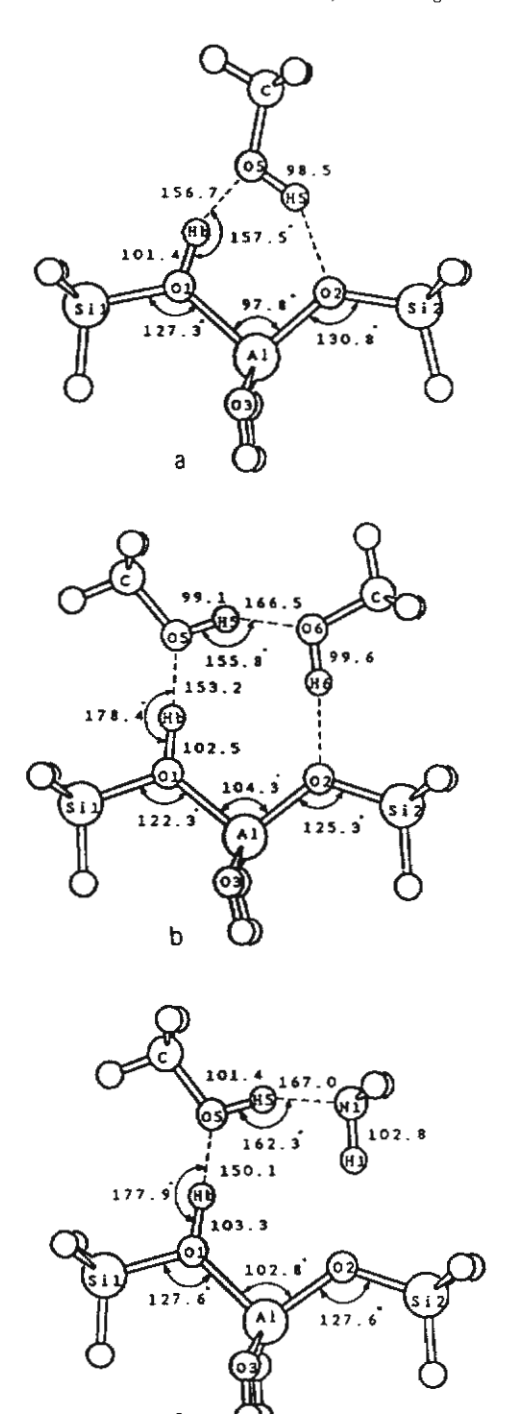


Fig. 3. Schematic representation of molecular models for the systems Brønsted acid site [H₂SiOHAl(OH)₂OSiH₃]; (H-Z): a) [H₃SiOHAl(OH)₂OSiH₃]/[CH₃OH]; b) [H₃SiOHAl(OH)₂OSiH₃]/[CH₃OH]; c) [H₃SiOHAl(OH)₂OSiH₃]/[CH₃OH][NH₃].

zeolitic proton onto the adsorbed ammonia. The Brønsted OH bonds of zeolitic catalysts are lengthened for the H-Z/[NH₃][CH₃OH] as compared to the corresponding binary complex of H-Z/[NH₃] (99.3 vs. 98.9 pm, see Fig. 1a,b).

3.1.2. Ion-pair formation

The optimized structure parameters of [H₃SiOAl (OH)₂SiH₃]⁷[NH₄][†], [H₃SiAl(OH)₂SiH₃]⁷[NH₄][†] [NH₃] and [H₃SiOAl(OH)₂SiH₃]⁷[NH₄][†] [CH₃OH] are reported. For the system [H₃SiOAl(OH)₂SiH₃]⁷ [NH₄][†], the ammonium cation forms two very strong hydrogen bonds towards the negatively charged zeolite (see Fig. 2a). The Al-O1, and Al-O2 distances are virtually equal and about 4.6 pm longer than that found in the anionic zeolite. For the high coverages, the ammonia is found to bond to the Bronsted acid site of H-Z, yielding ammonium cation, which operates as the centre site for further hydrogen bonding to methanol of ammonia (see Fig. 2b and 2c).

Attempts have been to observe the Z⁻[CH₃OH₂]⁺ [NH₃]; an initial structure with a methoxonium ion is optimized. The OH bond of [CH₃OH₂]⁺ and the hydrogen bond angle (O-H...N) in the complex is constrained at the optimized [CH₃OH₂]⁺ and 180°, respectively. However, during the optimization, the proton of [CH₃OH₂]⁺ is transferred to the ammonia molecule, and the final equilibrium complex H-Z/[CH₃OH][NH₄]⁺ is obtained. Note that this complex is achieved only at B3LYP, while only hydrogenbonded H-Z/[CH₃OH][NH₃] is obtained at the HF level of theory.

The energy for conversion of [H₃SiOHAl(OH)₂SiH₃]/[NH₃][CH₃OH] to [H₃SiOAl(OH)₂SiH₃]⁻/[NH₄]⁺[CH₃OH] is 0.74 kcal/mol. The details of the sorption processes were evaluated as follows. The coadsorption energy of ammonia and methanol on the cluster zeolite (H-Z) is the energy of reaction

$$H-Z+[NH_3]+[CH_3OH] \rightarrow H-Z/[NH_3][CH_3OH]$$
(1)

_....

Whilst for an anion (Z⁻) and ammonium cation (NH₄), the energies are those of the reactions

$$H - Z \rightarrow Z^- + H^+ \tag{2a}$$

$$NH_3 + H^+ \rightarrow [NH_4]^+ \tag{2b}$$

The energy for reaction (2a) is called the deprotonation energy and the protonation energy is represented by

Bond/pm or	H-Z[NH ₃]	H-ZINHAL	H-Z/INH, I[CH,OH]	Z./INH.I		Z-/[NII.] HNH.	NE	Z-/INH.] '[CH.,OH]	СН,ОН]
angic/ocg	HF	HF	HF	HF	взстр	НЕ	ВЗСУР	HF	взгур
A1-01	190.4	190.0	189.4	180.3	182.2	180.1	182.8	180.9	182.7
1-02	173.5	172.4	174.8	180.3	182.2	177.4	178.5	178.5	180.6
AI-03	172.2	172.5	172.4	173.1	174.2	173.6	175.1	173.6	174.8
9	172.2	172.5	172.4	173.1	174.2	173.6	175.1	173.6	174.8
< 0-17 >	177.1	176.8	177.2	176.7	178.2	176.2	6771	176.6	178.2
Si1-01	168.7	168.5	169.4	162.9	165.4	162.3	165.3	163.3	1991
2-02	161.5	160.2	163.7	162.9	165.4	160.6	163.4	162.6	165.0
I-Hb	6'86	99.4	99.3	1.67.7	157.7	163.7	149.7	158.7	148.9
I-H1	100.5	101.1	100.8	104.0	108.1	102.6	108.0	102.8	106.2
NI-N2	ı	321.0	ŧ	t	t	296.3	276.8	ı	ı
10-	271.4	272.7	272.0	263.4	258.4	267.4	260.0	264.4	259.6
-05	1	1	292.3	1	1	i	1	269.4	262.8
5-H5	1	1	95.4	1	1	1	1	96.4	8.66
Si1-01-A1	128.1	126.5	128.5	128.7	127.1	130.6	124.8	124.0	121.7
Si2-02-Al	140.6	153,7	128.7	128.6	127.0	131.9	125.7	124.7	122.8
01-A1-02	8'86	1.66	105.0	100.8	8.96	99.4	101.5	106.2	104.9
N1-H1-N2	1	171.2		1	1	161.7	173.5	1	ı
OI-HP-NI	171.6	171.1	170.5	150.8	152.5	170.3	176.6	1.77.1	179.6
20 111									

Table 2

Bond/pm or	.2		Z-H		н-х/сн,он]	H]	н-2/[СН,ОН],	OH] ₂	H-Z/CH30H][NH3]	[FHN][HC
angie/0eg	HF.	B31,YP	HF	B3LYP	H	ВЗГУР	HF	ВЗСУР	Ή	ВЗГУР
AI-01	176.1	177.6	194.4	194.7	191.3	190.8	190.2	189.3	190.7	189.4
A1-02	176.1	177.6	171.9	173.9	174.4	177.2	174.8	177.6	173.9	176.7
A103	176.4	177.7	171.6	173.1	171.9	173.4	172.2	173.7	172.3	174.0
A1-04	176.4	177.7	171.6	173.1	171.9	173.4	172.2	173.7	172.3	174.0
< AI-0 >	176.2	177.6	177.4	178.7	177.4	178.7	177.4	178.6	177.3	178.5
Si1-01	158.5	160.8	170.1	171.3	169.4	170.4	6.691	170.9	1.69.1	170.4
12-02	158.5	160.8	161.4	163.5	162.4	164.8	162.8	165.1	6.191	164.4
OI-Hb		ı	. 95,3	97.3	97.3	101.4	5.76	102.5	0.86	103.3
05-06	1	,	t	1	97.3	101.4	271.7	260.1	i	,
01-05	1	ı	í	ı	264.4	253,3	267.6	255.6	266.3	253.4
5-Hb	ı	ı	1	ı	170.7	156.7	170.8	153.2	169.0	150.2
O6-H6	ı	t	1	1	1	•	95.5	9.66	į	ı
05-H5	ι	ı	ı	1	95.4	98.5	6.7	99.1	5.96	101.4
Sil-Ol-Al	149.1	141.4	131.4	133.0	128.1	127.3	124.2	122.3	124.4	122.6
Si2-02-Al	149.1	141.4	152.3	146.9	135.5	130.8	128.8	125.3	134.8	127.6
01-A1-02	106.5	104.6	92.8	89.7	0.66	8'.26	104.	104.3	103.0	102.8
05-H5-06	ı	1	i	ı	ı	t	154.9	155.8	160.7	162.3
01-Hb-05	1	1	ŀ	1	160.5	157.5	171.7	178.4	171.4	177.9
NI-H6	ŧ	ı	1	,	ı	i	1	1	9:001	102.8
05-Mt	i	ı	1	t	i	ı	1	1	280.8	265.4
05-H5-M1	ı	,	ŀ	1	ı	,	i	t	160.7	162.3

reaction (2b). For an ion-pair, Z⁻/[NH₄] [CH₃OH], the complexation energy is the energy of the reaction

$$[Z^{-}]+[NH_{4}]^{+}+[CH_{3}OH] \rightarrow Z^{-}/[NH_{4}]^{+}[CH_{3}OH]$$

Finally, the conversion energy of a covalent structure to an ion-pair structure is the sum of the energies of the three reactions above, i.e.

 $H-Z/[NH_3][CH_3OH] \rightarrow Z^-/[NH_4]^+[CH_3OH]$ (4) The reaction energies of each step are summarized in the schematic diagram in Scheme 1. From the reaction energies (see Table 4) of all the complexes, we can propose the reaction mechanism of coadsorption of methanol and ammonia on H-Z as depicted in Scheme 2.

3.2. Coadsorption of methanol and ammonia on Na-zeolites (Na-Z)

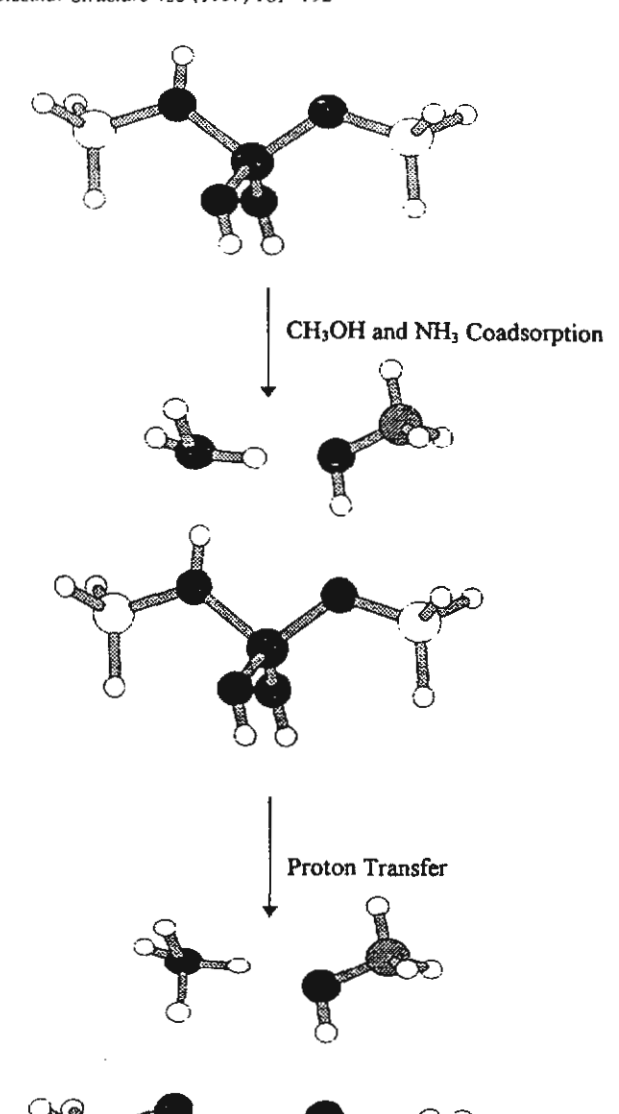
The effect of the cation on the structure of zeolitic catalysts and the coadsorption process is investigated at B3LYP/6-31G* and HF/6-31G* levels of theory. The fully optimized geometry structures for Na-Z, Na-Z/[NH₃], Na-Z/[CH₃OH], Na-Z/[NH₃][CH₃OH] and Na-Z/[CH₃OH][NH₃] are documented in Table 3.

3.2.1. The Na(1)/zeolite complex

The Na(I) does not bind with a particular bridging oxygen atom in the [AlO₄]⁻ but is symmetrically bidentated to the O1 and O2 of the [AlO₄]⁻ tetrahedron and the interaction has ionic character. The symmetric binding between Na(I) and [AlO₄]⁻ has been confirmed by an ESR experiment [34]. The optimized Na(I)...O distance is found to be 216.0 pm and the corresponding energy is 134.09 kcal mol⁻¹. Table 3 further indicates that the charge compensating Na(I) can affect the ≡Si-O-Al≡ by weakening the Si-O and Al-O bonds, as compared to the anionic framework (see Table 2).

H-Z+[NH₃]+[CH₃OH]
$$\xrightarrow{97.99}$$
 Z'+[NH₄]++[CH₃OH]
(i) 22.42 (iii) -119.67
H-Z/[NH₃][CH₃OH] $\xrightarrow{0.74}$ Z'/[NH₄]+[CH₃OH]

Scheme 1.



Scheme 2.

3.2.2. The Na-Z/[CH3OH] complex

The optimized Na(I)...O(Z) distance in the Na-Z/[CH₃OH] complex is 2.8 pm larger than in the Na(I)/zeolite complex. The Na...O(m) equilibrium distance of the Na-Z/[CH₃OH] complex is about 7.7 pm longer than the corresponding distance in the isolated Na(I) complex, Na(I)/[CH₃OH], in

Table 3
HF/6-31G* and B3LYP/631G* optimized structure parameters for H₃SiONaAl(OH)₂OSiH₃, H₃SiONaAl(OH)₂OSiH₃/[CH₃OH], H₃SiONaAl(OH)₂OSiH₃/[CH₃OH], H₃SiONaAl(OH)₂OSiH₃/[CH₃OH][NH₃] and H₃SiONaAl(OH)₂OSiH₃/[CH₃OH]

	Z-gN		Na-Z/(NH)	-=	Na-Z/CH OH	OHI	Na-Z/[NH	Na-Z/[NH], IICH, OH]	Na-Z/CH	Na-Z/[CH,OH][NH,]
angio ock	HF	B3LYP	HF	B3LYP	표	B3LYP	HF	взгур	Ή	B3LYP
AI-01	180.3	182.0	179.8	181.5	179.8	181.5	179.6	181.2	179.6	181.3
N-02	180.4	182.0	179.8	181.4	179.8	181.6	179.8	181.4	179.7	181.2
1-03	172.8	174.1	.173.1	174.4	173.1	174.4	173.1	174.4	173.1	174.5
50	172.8	174.1	173.1	174.4	173.1	174.4	173.1	174.4	173.1	174.5
< 0-14 >	176.6	178.0	176.4	177.9	176.4	178,0	176.4	177.8	176.4	177.9
IO-1	162.8	164.9	162.3	164.4	162.3	164.5	162.3	10-17-1	162,3	162,4
2-02	162.8	164.9	162.3	164.4	162.3	164.4	161.7	163.5	161.7	163.6
1-H1	ı	ŀ	100.5	102.1	ı	1	100.8	10.28	100.4	102.0
01-05	,	ı	ı	ţ	424.0	420.8	ì	ı	438.7	436.9
- 2	ŧ	t	439.0	433.0	ı	1	450.9	449.2	ì	ı
N-N-	1	ı	t	ı	ı	,	310.6	298.6	289.0	276.9
-Na	217.6	216.0	220.9	219.5	220.6	219.1	221.7	220.7	221.7	220.6
I-Na	ı	t	242.3	238.8	1	1	239.6	235.7	ı	i
5-Na	ı	ı	ı	ı	227.8	225.7	ı	t	223.6	220.6
S-H5	ı	ì	I	ı	94.8	6'96	94.8	97.0	96.4	100.3
Si1-01-Al	129.8	127.5	131.0	128.6	131.1	128.5	131.4	129.0	131.1	128.8
2-02-AI	130.1	127.6	131.0	128.6	131.1	128.6	132.0	130.5	132.1	130.4
01-AI-02	96.5	94.9	97.1	95.5	97.0	96.6	97.1	95.5	97.2	95.7
01-Na-05	ı	ŧ	1	ı	142.0	142.2	i	1	160.3	170.0
I-Na-NI	1	1	142.7	141.7	1	t	155.7	159.7	ı	ı
05-H5-NI	ŀ	ı	i	ı	i	ı	ı	ı	176.0	175.0
N1-H1-05			1		,	ŀ	168.7	168.8	ı	•

accordance with the lower binding energy; $\Delta E(\text{Na(I)/CH}_3\text{OH}) = -31.08 \text{ kcal mol}^{-1}$, $\Delta E(\text{Na-Z/CH}_3\text{OH}) = -18.39 \text{ kcal mol}^{-1}$.

One point of interest is that the Na-Z/[CH₃OH] leads to an increased positive charge for the methanol hydrogen by about 0.0462. This suggests that the ability of the methanol molecule to form a hydrogen bond as a proton-donor molecule is enhanced with Na-Z attached to the methanol oxygen atom. We note that the absolute values from Mulliken population analysis are not very reliable, and also depend on the basis set employed. However, within closely related structures a useful value will be yielded.

3.2.3. The Na-Z/[CH₃OH][NH₃] complex

The changes in structural parameters of the coadsorption complexes Na-Z/[CH₃OH][NH₃] are in agreement with Gutmann's rule [33], i.e. a lengthening of the methanol OH bond, a shortening of Na...O(m), a lengthening of Na...O(Z), and a shortening of the Al-O (adjacent to sodium atom) and Si-O bonds, as illustrated in Fig. 4c. The optimized Na(I)...O(m) distance in the Na-Z/[CH₃OH][NH₃] is 5.1 pm smaller than in the Na-Z/[CH₃OH] complex, where O(m) and O(Z) denote methanol oxygen and oxygen of zeolite, respectively. The rotational energy barrier around the O-H...N bond of the Na-Z/[CH₃OH][NH₃] complex is lower than KT. Thus Na-Z does not seem to hinder the free rotation of the ammonia molecule.

Another additional point of interest is that the OH...N distance is contracted from the 289.2 pm found in the H-bonded dimers of CH₃OH...NH₃ to 276.9 pm for Na-Z/[CH₃OH][NH₃]. This reduced O-H...N distance reflects an increase of binding energy due to the Na-Z. This can also be simply rationalized on the basis of the hydrogen atom population. The Na-Z leads to a decrease in electron density at the methanol proton in the Na-Z/[CH₃OH][NH₃] of 0.1088 units, compared to 0.0588 units in the CH₃OH...NH₃.

From the reaction energies in Table 4, the reaction mechanism may be proposed as depicted in Scheme 3.

Fig. 4. Schematic representation of molecular models for the systems: a) $[H_3SiONaAl(OH)_2OSiH_3]$; [Na-Z); b) $[H_3SiONaAl(OH)_2OSiH_3]$ / $[CH_3OH]$; c) $[H_3SiONaAl(OH)_2OSiH_3]$ / $[CH_3OH]$ [$[NH_3]$.

Table 4
Computed binding energies

Systems	Binding energy	y (– Δ <i>E</i> /kcał mol ⁻¹)
	HF/6-31G*	B3LYP/6-31G*
[H ₃ SiOHAl(OH ₂)OSiH ₃]/ [CH ₃ OH]	13.50	18.48
[H ₃ SiOHAl(OH ₂)OSiH ₃)/ [CH ₃ OH] ₂	21.51	29.60
[H ₃ SiOHAl(OH ₂)OSiH ₃]/ [CH ₃ OH][NH ₃]	22.13	31.64
[H ₃ SiOHAl(OH ₂)OSiH ₃]/ [NH ₃]	15.81	-
[H ₃ SiOAl(OH ₂)OSiH ₃]/ [NH ₄] ⁺	112.25	120.96
[H ₃ SiOHAl(OH ₂)OSiH ₃]/ [NH ₃] ₂	21.47	-
(H ₃ SiOAt(OH ₂)OSiH ₃)/ [NH ₄)*(NH ₃]	120.08	130.02
[H ₃ SiOHAl(OH ₂)OSiH ₃]/ [NH ₃][CH ₃ OH]	22.42	-
[H ₃ SiOAl(OH ₂)OSiH ₃]/ [NH ₄]*[CH ₃ OH]	119.67	131.59
[H ₃ SiONaAl(OH ₂)OSiH ₃]/ [NH ₃]	19.72	21.57
[H ₃ SiON ₂ AI(OH ₂)OSiH ₃]/ [NH ₃][CH ₃ OH]	27.07	31.03
[H ₃ SiONaAl(OH ₂)OSiH ₃]/ [CH ₃ OH]	17.33	18.39
[H ₃ SiON ₂ Al(OH ₂)OSiH ₃]/ [CH ₃ OH][NH ₃]	30.34	35.76

Scheme 2 and Scheme 3 indicate that when the methanol and ammonia are coadsorbed, the methanol preferentially adsorbs on Na-Z, while the ammonia binds favorably to H-Z. Our findings are in excellent agreement with very recent experimental data [23].

4. Conclusion

We have carried out HF and B3LYP methods with 6-31G* basis set to investigate the coadsorption of methanol and ammonia on H-zeolities (H-Z) and alkaline-exchanged zeolites (Na-Z). Comparing HF and B3LYP results with available experimental data, the B3LYP yields structural parameters which are in good agreement with experimental data. The Al...H distance of zeolite has been estimated experimentally as 238 ± 4 pm, whereas our B3LYP value is 239.7 pm.

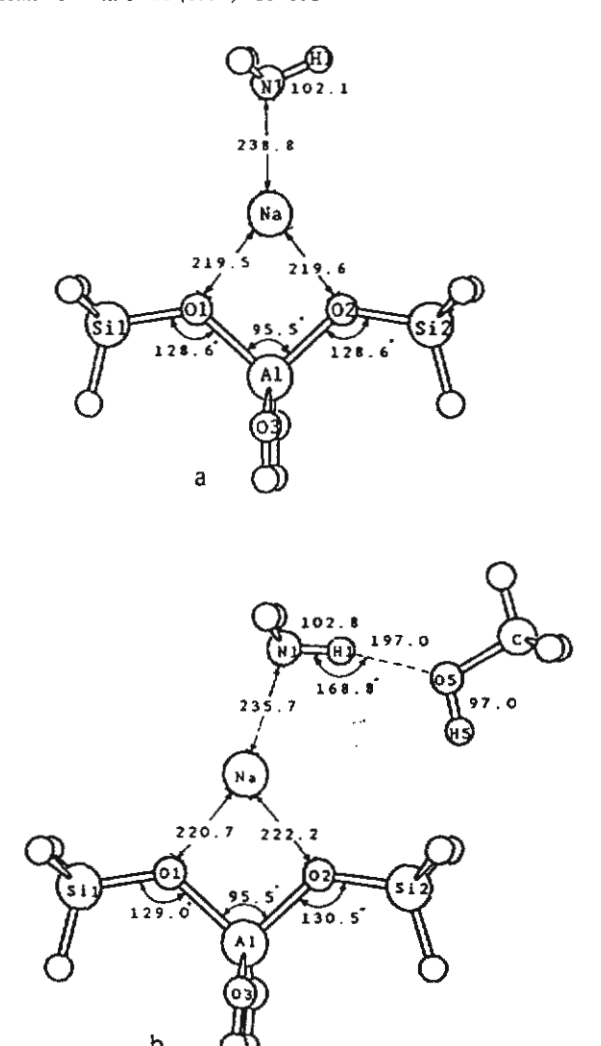
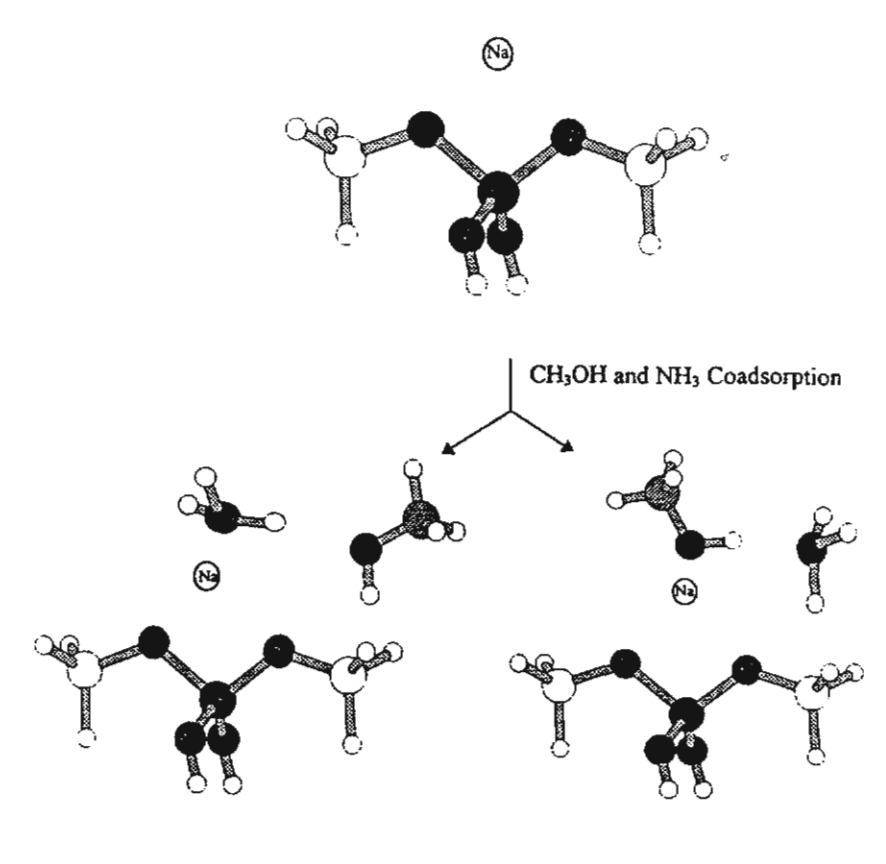


Fig. 5. Schematic representation of molecular models for the systems: a) [H₃SiONaAl(OH)₂OSiH₃]/[NH₃]; b) [H₃SiONaAl(OH)₂OSiH₃]/ [NH₃][CH₃OH].

A comprehensive study of the coadsorption of absorbate molecules with the surface hydroxyl reveals several interesting points. Structure Na-Z/[CH₃OH][NH₃] is lower in energy than Na-Z/[NH₃][CH₃OH], which suggests that the former is more favourable in the coadsorption process. The reaction mechanism of coadsorption of methanol and ammonia on H-Z is that the ammonia is found to stabilize to the Brønsted acid site of H-Z, generating an ammonium cation, which acts as an active site for methanol.



 $\Delta E = -31.03 \text{ kcal/mol}$

 $\Delta E = -35.76 \text{ kcal/mol}$

Scheme 3.

The results obtained in the present study are very useful from the experimental point of view, since the adsorption and coadsorption processes on the surface site are found to play a significant role in catalytic processes.

Acknowledgements

This work was supported by donors of the Thailand Research Fund (TRF) in supporting the research career development project (The TRF research scholar) and the Kasetsart University Research and Development Institute (KURDI). Our sincere thanks are due to Professor R. Ahlrichs (Karlsruhe, Germany) for his continued support of this work.

References

- [1] J. Klinowski, Chem. Rev. 91 (1991) 1459.
- [2] J.M. Thomas, Sci. Am. 266 (1991) 82.
- [3] G.J. Kramer, R.A. van Santen, C.A. Emeis, A.K. Nowak, Nature 363 (1993) 529.
- [4] E. Kassab, J. Fouquet, M. Allavena, A.M. Evleth, J. Phys. Chem. 97 (1993) 9034.
- [5] C.T.W. Chu, C.D. Chang, J. Phys. Chem. 89 (1985) 1569.
- [6] M.A. Makarova, S.P. Bates, J. Dwyer, J. Am. Chem. Soc. 117 (1995) 11309.
- [7] J. Das, C.V.V. Satyanaryana, D.K. Chakrabarty, S.N. Piramanayagarn, S.N. Shringi, J. Chem. Soc., Faraday Trans. 88 (1992) 3255.
- [8] S.R. Blazkowski, R.A. van Santen, J. Phys. Chem. 99 (1995) 11728.
- [9] H.J. Soscun, P.J. Omalley, A. Hinchcliffe, J. Mol. Struct. (Theochem) 341 (1995) 237.
- [10] J. Limtrakul, S. Pollman-Hannongbua, J. Mol. Struct. (Theochem) 280 (1993) 139.

- [11] J. Limtrakul, J. Mol. Struct. 288 (1993) 105.
- [12] J. Limtrakul, J. Yoinuan, D. Tantanak, J. Mol. Struct. 312 (1994) 183.
- [13] J.A. Zygmunt, L.A. Curtiss, L.E. Iton, M.K. Erhardt, J. Phys. Chem. 100 (1996) 6663.
- [14] M. Krossner, J. Sauer, J. Phys. Chem. 100 (1996) 6199.
- [15] F. Haase, J. Sauer, J. Am. Chem. Soc. 117 (1995) 3780.
- [16] J. Limtrakul, Chem. Phys. 193 (1995) 79.
- [17] J. Sauer, P. Ugliehgo, E. Garrone, V.R. Saunders, Chem. Rev. 94 (1994) 2095.
- [18] G. Mirth, J.A. Lercher, M.W. Anderson, J. Klinowski, J. Chem. Soc. Faraday Trans. 86 (1990) 3039.
- [19] R.A. van Santen, G.J. Kramer, Chem. Rev. 95 (1995) 637.
- [20] S.L. Meisel, J.P. McCullogh, C.H. Lechthaler, P.B. Weisz, Chem. Tech. 6 (1976) 86.
- [21] E. Nusterer, P.E. Blochl, K. Schwarz, Angew. Chem. Int. Ed. Eng. 35 (1996) 175.
- [22] W.E. Farneth, R.J. Gorte, Chem. Rev. 95 (1995) 615.
- [23] A. Kogelbauer, G. Grundling, J.A. Lercher, J. Phys. Chem. 100 (1996) 1837-1852.
- [24] J. Limtrakul, P. Treesakol, Chem. Phys. 215 (1997) 77.

- [25] J. Limtrakul, D. Tantanak, J. Mol. Struct. 358 (1995) 179.
- [26] J. Limtrakul, D. Tantanak, Chem. Phys. 208 (1996) 331.
- [27] Frisch, M.J., Trucks, G.W., Schlegel, H.B., Gill, P.M.W., Johnson, B.G., Wong, M.W., Foresman, J.B., Robb, M.A., Head-Gordon, M., Replogle, E.S., Gomperts, R., Andres, J.L., Raghavachari, K., Binkley, I.A., Gonzalez, C., Martin, R.L., Fox, D.J., DeFrees, D.J., Baker, J., Stewart, J.J.P., Pople, J.A., Gaussian 94 (Gaussian Inc., Pittsburgh, 1994).
- [28] R. Ahlrichs, R. Baer, M. Haeser. H. Horn, C. Koemel, Chem. Phys. Lett. 162 (1989) 165.
- [29] M. Haeser, R. Ahlrichs, J. Comput. Chem. 10 (1989) 104.
- [30] J. Almtoef Jr, K. Faegri, K. Korsell, J. Comput. Chem. 3 (1982) 385.
- [31] J.A. Pople, D.L. Beveridge, Approximate Molecular Orbital Theory, McGraw-Hill Inc., New York, 1970.
- [32] D. Freude, J. Klinowski, H. Hamdan, Chem. Phys. Letters 149 (1988) 355.
- [33] V. Gutmann, The Donor-Acceptor Approach to Molecular Interactions, Plenum Press, New York, 1978.
- [34] H. Hozono, H. Kawazoc, J. Nishii, J. Kanazawa, J. Non-Cryst. Solid 51 (1982) 217.

Structure and Reaction Pathways for Methylamine/Zeolite System

Jumras Limtrakul and Mayuso Kuno

Laboratory for Computational & Applied Chemistry, Chemistry Department, Faculty of Science, Kasetsart University, Bangkok 10900/THAILAND; fscijrl@ku.ac.th

ABSTRACT

Reaction pathways of methylamine synthesis from methanol and ammonia on zeolite (ZOH) have been carried out using Hartree-Fock (HF) and density functional theory (DFT) approaches. Structures of the adsorption reactants, transition states, intermediates, and adsorption products were optimized at DFT(B3LYP) and HF levels of theory using 6-31G(d). Four different reaction pathways, including Langmuir-Hinshelwood (methanol and ammonia are both bound to Brønsted acid sites) and Eley-Rideal (two adsorbing molecules react; methanol is unbound, the ammonia is bound to a Brønsted acid site) mechanisms of methylamine production, were investigated. The reaction pathway which involves dehydration of one methanol and generating surface methoxy species was found to possess a substantially higher activation energy barrier. The lower corresponding energy was estimated for methoxy-zeolite formation from coadsorption of CH₃OH and NH₃ at Brønsted acid sites. The reaction pathways involving an associative reaction were, however, found to be more preferable in methylamine formation.

INTRODUCTION

For many years, zeolites have been found in industrial applications as catalysts in petrochemical processes, because of their unique catalytic activity, excellent selectivity as well as superior stability in many important conversions and upgrading processes as compared to other materials [1]. The acidity of zeolitic catalysts released from the surface hydroxyls (\equiv Si-OH-Al \equiv) is responsible for catalytic function [2-3]. The structure of such catalytic sites and their mode of interaction with simple adsorbates have been investigated as a crucial step in elucidating the catalytic reaction mechanism occurring at these active sites.

Of particular interest in this active research is the products generated from the adsorption of methanol (i.e., conversion of methanol to gasoline) and the coadsorption of methanol and ammonia (the production of methylamines which are essential chemical building subunits for important industrial materials such as resins, fibers, dyes and pharmaceuticals) [4]. One of the crucial steps of these chemically interesting systems involves the adsorption of probed molecules on the catalyst surface.

Structure and Reaction Pathways for Methylamine/Zeolite System

Jumras Limtrakul and Mayuso Kuno

Laboratory for Computational & Applied Chemistry, Chemistry Department, Faculty of Science, Kasetsart University, Bangkok 10900/THAILAND; fscijrl@ku.ac.th

ABSTRACT

Reaction pathways of methylamine synthesis from methanol and ammonia on zeolite (ZOH) have been carried out using Hartree-Fock (HF) and density functional theory (DFT) approaches. Structures of the adsorption reactants, transition states, intermediates, and adsorption products were optimized at DFT(B3LYP) and HF levels of theory using 6-31G(d). Four different reaction pathways, including Langmuir-Hinshelwood (methanol and ammonia are both bound to Brønsted acid sites) and Eley-Rideal (two adsorbing molecules react; methanol is unbound, the ammonia is bound to a Brønsted acid site) mechanisms of methylamine production, were investigated. The reaction pathway which involves dehydration of one methanol and generating surface methoxy species was found to possess a substantially higher activation energy barrier. The lower corresponding energy was estimated for methoxy-zeolite formation from coadsorption of CH₃OH and NH₃ at Brønsted acid sites. The reaction pathways involving an associative reaction were, however, found to be more preferable in methylamine formation.

INTRODUCTION

For many years, zeolites have been found in industrial applications as catalysts in petrochemical processes, because of their unique catalytic activity, excellent selectivity as well as superior stability in many important conversions and upgrading processes as compared to other materials [1]. The acidity of zeolitic catalysts released from the surface hydroxyls (\equiv Si-OH-Al \equiv) is responsible for catalytic function [2-3]. The structure of such catalytic sites and their mode of interaction with simple adsorbates have been investigated as a crucial step in elucidating the catalytic reaction mechanism occurring at these active sites.

Of particular interest in this active research is the products generated from the adsorption of methanol (i.e., conversion of methanol to gasoline) and the coadsorption of methanol and ammonia (the production of methylamines which are essential chemical building subunits for important industrial materials such as resins, fibers, dyes and pharmaceuticals) [4]. One of the crucial steps of these chemically interesting systems involves the adsorption of probed molecules on the catalyst surface.

In spite of a large number of documents about zeolite research, the details of structures and reaction mechanisms of adsorption [2,5-8], and particularly of coadsorption [9] are still incomplete and only partially solved.

METHODS

We employed the adsorption clusters illustrated in Figure 1-5 as the models of all possible adsorption reactants: [XOHAl(OH)₂OX]/[CH₃OH], [XOHAl(OH)₂OX]/[CH₃OH][NH₃], [XOHAl(OH)₂OX]/[NH₃] [CH₃OH]; adsorption surface methoxy intermediates, [XOCH₃Al(OH)₂OX]/[NH₃], [XOCH₃Al(OH)₂OX]/[H₂O]; transition state complexes, and adsorption products, [XOHAl(OH)₂OX]/[CH₃NH₂], [XOHAl(OH)₂OX]/[CH₃NH₂], [XOHAl(OH)₂OX]/[CH₃NH₂], where X=H and SiH₃, hereafter referred to as 1T and 3T cluster models for HOHAl(H)₂OH and H3SiOHAl(H)₂OSiH₃, respectively.

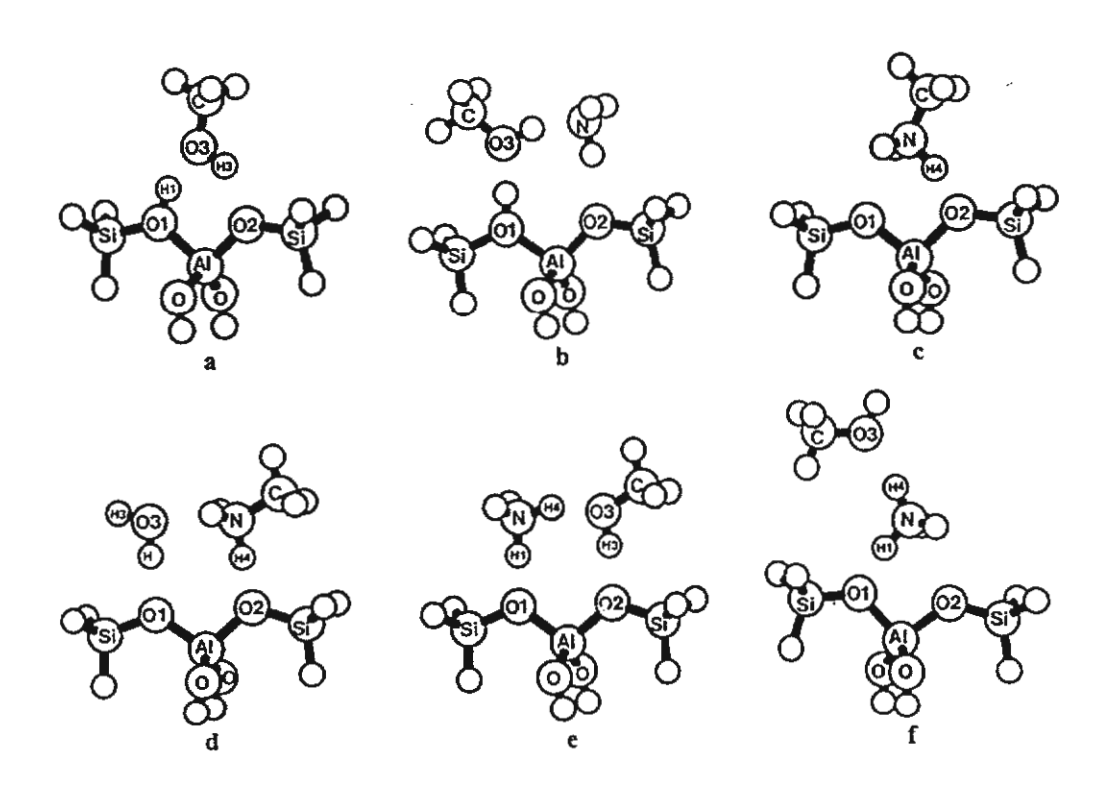


Figure 1. Optimized structures for different adsorption complexes (H₃SiOHAl(OH)₂OSiH₃ (3T), H₃SiOHAl(OH)₂OSiH₃/CH₃OH (1a), H₃SiOHAl(OH)₂OSiH₃/CH₃OH/NH₃ (1b), [H₃SiOAl(OH)₂OSiH₃]⁻/[CH₃NH₃]⁺/H₂O (1d), [H₃SiOAl(OH)₂OSiH₃]⁻/CH₃OH/[NH₄]⁺ (1e), [H₃SiOAl(OH)₂OSiH₃]⁻/[NH₄]⁺/CH₃OH/ (1f)) at B3LYP/6-31G(d) level of theory.

Full geometry optimization of the cluster models mentioned above was carried out with the DFT methods employing B3LYP density functional. This functional has been recently

demonstrated to yield accurate results about molecular structures, and vibrational frequencies for zeolites [10-11]. Transition state searches were performed using an eigenvalue-following algorithm [12]. On each optimized cluster, a vibrational analysis was made in order to obtain the normal modes. Final energies of some adsorption complexes were improved from point calculations at B3LYP/6-311+G(3df,2p) theoretical level. All density functional computations were performed using the program Gaussian-94 [13].

For the HF calculations, we employed the TURBOMOLE code [14] which is based on the direct SCF method. Geometry optimization was terminated when the gradient norm with respect to internal coordinates was less than 10^{-3} E_h/a₀. The energy change was then below 5×10^{-6} a.u.

The computations were carried out using DEC Alphastation 250 and HP 9000/700 workstations at the Laboratory for Computational and Applied Chemistry at Kasetsart University.

RESULTS AND DISCUSSION

Four different reaction pathways of methylamine synthesis have been investigated, as depicted in Figures 2-5.

The first reaction pathway for methylamine formation: One methanol molecule is adsorbed on the catalyst surface to yield ZOCH₃, followed by the interaction of ammonia to yield MeNH₂.

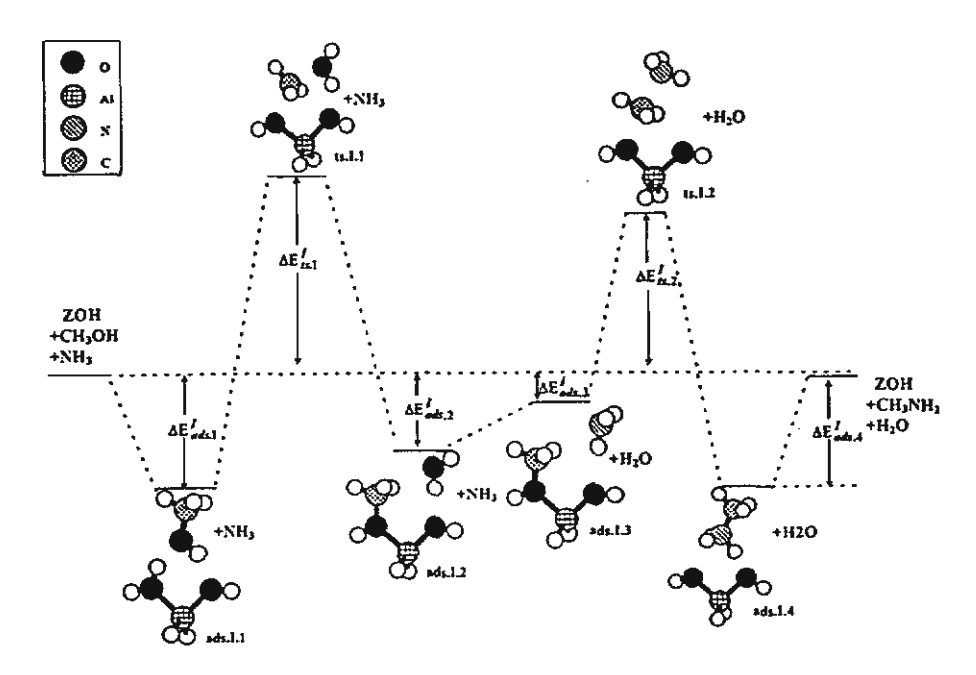


Figure 2. Path I: One CH₃OH is adsorbed on ZOH, ZOCH₃ generated, and the interaction of NH₃ with ZOCH₃ to yield methylamine.

The first reaction mechanism involves only one CH₃OH molecule adsorbed on the zeolitic acid site, ZOH/CH₃OH (see ads.I.1, Figure 2) which is then dehydrated and leaves a methyl group attached to the zeolite basic oxygen, ZOCH₃.

The adsorption energies of ZOH/CH₃OH were found to be -56.48 and -77.32 kJ/mol for 3T cluster models at HF and B3LYP levels of theory, respectively, which is in agreement with other theoretical values ranging from -56 to -89 kJ/mol [2,7,8] depending on the method and cluster size employed. Sauer's HF estimate of the adsorption energy of the large cluster (11T model fragment of faujasite) was -83.0 kJ/mol after correction for electron correlation, ZPE and BSSE. Experimental estimates of the heat of adsorption in acidic zeolites range from -63 [15] and -110 to -120 kJ/mol [referenced in ref. 2].

Parameters	3 <u>T</u>	la	lb	lc	ld	le	lf
Al-01	194.67	190.80	189.45	179.55	180.01	182.70	182.71
Ai-O2	173.89	177.18	176.69	183,14	182.78	180.57	179.35
O1-H1	97.30	101.36	103.34	-	173.52	148.87	151.13
01-03	-	253.28	253.45	-	272.72	382.63	461.78
O2-O3	-	267.96	372.47	-	398.68	267.46	553.16
O3-H3	-	98.48	101.38	-	96.74	99.84	96.81
01-N	-	-	406.18	263.98	361.00	- 259.68	259.27
O2-N	-	-	299.77	256.69	260.72	379.21	268.22
03-N	-	-	265.38	-	258.72	262.75	284.99
O2-H3	-	181.22	340.31	-	487.34	168.09	620.88
O2-H4	-	-	197.82	147.55	150.89	333.32	371.66
N-HI	-	-	331.31	-	274.99	110.81	109.61
N-H4	-	-	102.81	110.77	109.87	106.16	103.57
O1-A1-O2	89.66	97.84	102.83	97.88	103.20	104.86	98.23
O1-H1-O3	-	157.51	177.90	-	175.70	116.14	139.10
01-H1-N	-	•	130.57		105.20	179.56	167.71
O2-H3-N	-	-	61.73	-	31.27	108.71	-
O2-H4-N	-	-	170.82	166.96	178.00	107.62	-
O3-H4-N	-	~	70.34	-	59.45	159.99	172.32
Al-O1-HI	-	113.35	122.80	-	131.69	125.00	105.94
Al-O2-H4	-	-	131.03	105.78	120.04	.96.47	99.44
AI-O1-O3	-	98.22	124.04	-	130.12	81.58	134.47
AI-02-N	-	-	127.89	100.19	120.88	80.99	98.50
-ΔE (kJ/mol)		77.31	132.40	101.61	151.27	148.04	132.80

Table 1: Optimized structure parameters (distances in pm and angles in deg.) and binding energies (kJ/mol) for different adsorption complexes (cf. Figure 1).

The activation energy, ΔE_{sct}^{I} , is quite high, +245.79 kJ/mol. However, this value compares well with the results of Sinclair and Catlow [5] 250 and 244 kJ/mol at the DFT/DZVP and DFT/DZVP levels of theory, respectively. The high value of ΔE_{sct}^{I} indicates that this catalytic route may therefore only play a minor role in methanol activation over acidic zeolites. A similar conclusion for DME formation from methanol has been noted by Catlow group [5].

The optimized geometrical parameters of zeolitic clusters with methylamine are reported for the first time and summarized in Table 1. The results for the surface complex cluster indicate that the adsorbed methylamine interacts strongly with the Brønsted acid sites of zeolite and form protonated methylamine cation, [CH₃NH₃]⁺, on the catalytic surface with the adsorption energy of -101.61 kJ/mol. The change in the structural parameters of zeolite upon complexation with methanol are impressive. The results are in line with Gutmann's rule [16], i.e. a lengthening of the bridging O-H bond, a shortening of Al-O adjacent to this bond, and a lengthening of Al-O (not adjacent to it).

The intermolecular O-H...N hydrogen bond in the ZOH/MMA complex, [H₃SiOAl(OH)₂OSiH₃][†], is evaluated to be 256.69 pm, less than that found in the neutral complexes. The contracted intermolecular distance of the complex reflects an increase of the binding energy (-101.61 versus -83.56 kJ/mol). The energy for conversion of [H₃SiOAl(OH)₂OSiH₃]/[CH₃NH₃][†] to [H₃SiOHAl(OH)₂OSiH₃]/[CH₃NH₂] is -18.05 kJ/mol. The result implies that the desorbed CH₃NH₂ is difficult to generate without the help of other adsorbates, e.g. NH₃ molecules in this study.

The second reaction pathway for methylamine formation: Simultaneous adsorption of CH₃OH and NH₃ on ZOH generating TS structure for methylamine formation.

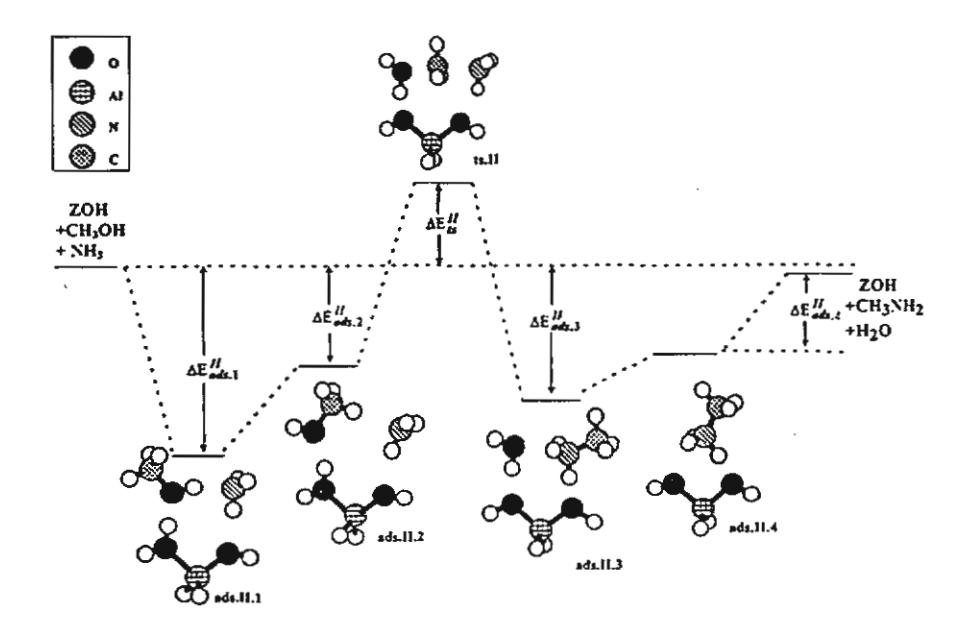


Figure 3. Path II: Simultaneous adsorption of CH₃OH and NH₃ on ZOH, generating a transition state structure for methylamine formation.

Structures of adsorption reactants, adsorption surface methoxy intermediates, and the adsorption products are shown in Figure 3. Selected optimized geometrical structures are tabulated in Table 1.

The starting adsorption reactants involve methanol and ammonia simultaneously adsorbed on ZOH (ads.II.1 in Figure 3). The adsorption energy ($\Delta E_{ads.II.1}^{II}$) for this adsorption complex is found to be -132.40 kJ/mol. Although no identical system has been published so far, our calculated adsorption energy, $\Delta E_{ads.II.1}^{II}$, of chemically different admolecules of methanol and ammonia should be compared also to the adsorption energy of chemically identical admolecules of two methanol molecules (-123.85 kJ/mol (B3LYP) for 3T/[CH₃OH]₂). These energy values can also be compared to the initial théoretical investigations of adsorption energy of two methanol molecules at the zeolitic surface [2,7-8]. Gale's DFT/BLYP estimated adsorption energy of the two methanols was -119.16 kJ/mol for 4Tcluster model [8]. Limtrakul [7] reported similar adsorption energies of -56.48 kJ/mol for the first and -35.52 kJ/mol for the second methanol from calculations at the HF theoretical level.

In order to search for the transition state complex of methylamine formation, the preferred configuration, (ads.II.2, Figure 3), has to be selected. This adsorption complex, ads.II.2, can be achieved by rotating the methanol molecule in such a way that the methyl group can be attached by the nucleophile, NH₃. The structure of transition state may be derived from the S_N2 reaction between the methoxonium cation and nucleophile NH₃. The activation energy barrier related to the adsorption complex, ads.II.2 is evaluated to be -126.09 kJ/mol, which is less stable than the ads.II.1 by 57.47 kJ/mol. The overall activation energy barrier related to the ads.II.1 for this reaction route becomes 183.56 kJ/mol. The activation energy at B3LYP/6-311G+(3df,2p)//B3LYP/6-31G(d) level of theory was 171.98 kJ/mol, which is about 12 kJ/mol lower than the fully optimized B3LYP/6-31G(d) structure.

The third reaction pathway for methylamine formation: Methanol and Ammonia are simultaneously adsorbed on ZOH generating ZOCH₃, which interacts with the ammonia promoter to yield methylamine.

The side-on MeOH/NH₃ adsorption, ads.III.2 (Figure 4) is supposed to be the precursor for the formation of surface methoxy intermediate, ads.III.4, which may further interact with ammonia to yield methylamine. However, the most stable adsorption reactants, ads.III.1, where ammonia is adsorbed on the zeolitic acid site, is about 40 kJ/mol more stable than the side-on MeOH/NH₃ adsorption (ads.III.2). The ΔE_{set}^{III} which is related to ads.III.1 is found to be 197.10 kJ/mol. This activation energy barrier is very much lower than ΔE_{set}^{I} obtained from the first type of reaction pathway. It is clearly due to the lesser strain in the transition-state structure, ts.III.1. The three-center angle of the transition-state structure is calculated to be ca. 170°, which is close to the optimum angle of 180° for an S_N2 mechanism. The result indicates that the influence of the adsorbed ammonia is to significantly decrease ΔE_{set}^{III} , which enhances the methylation reaction. Due to the lower activation energy, ΔE_{set}^{III} , as compared to ΔE_{set}^{II} of the first reaction route, this reaction route may play a significant role in methylamine synthesis.

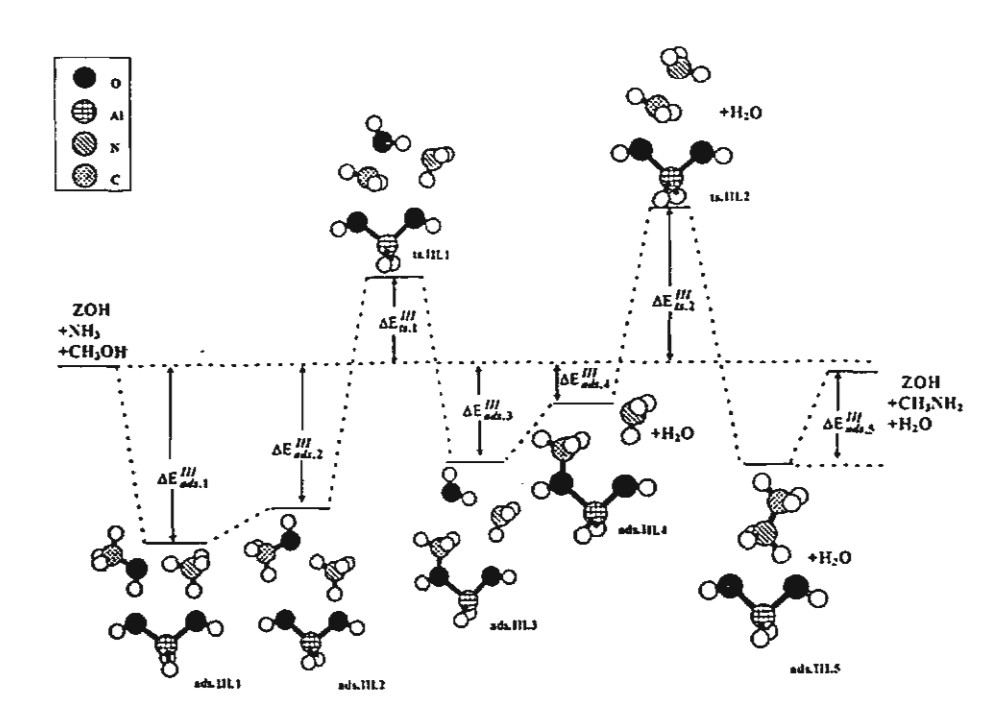


Figure 4. Path III: Both CH₃OH and NH₃ are adsorbed on ZOH, ZOCH₃ is generated via S_N2 with the help of the promoter NH₃, and the interaction of NH₃ with ZOCH₃ to yield methylamine formation.

The fourth reaction pathway for methylamine formation: Eley-Rideal mechanism where only NH₃ is adsorbed on the Brønsted acid site, followed by CH₃OH binding to the adsorbed NH₃, generating TS structure.

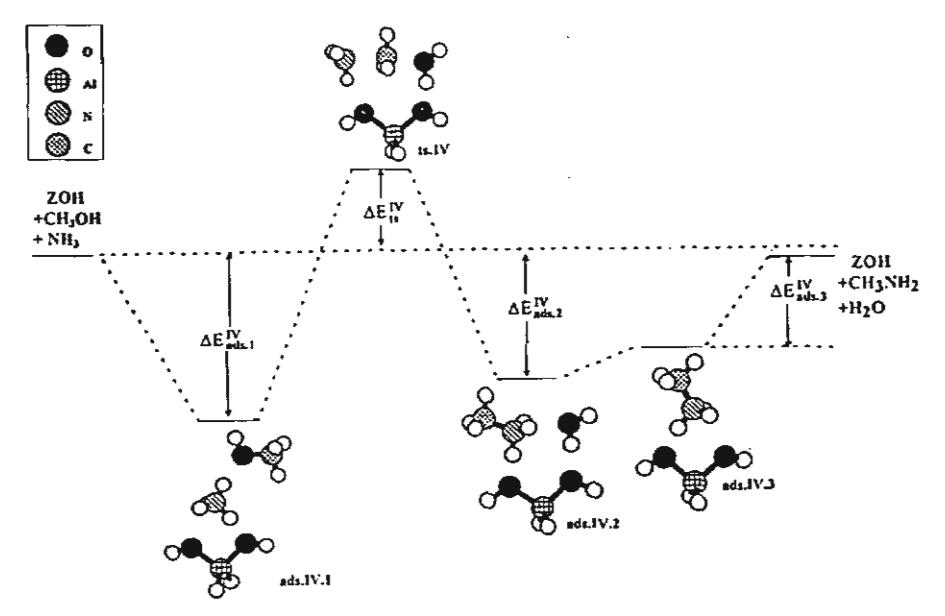


Figure 5. Path IV: Only NH₃ is adsorbed on the Brønsted acid site, CH₃OH is bound to the adsorbed NH₃, generating transition state structure which is converted to methylamine formation.

The aforementioned second and third reaction pathways, which involve the binding of both methanol and ammonia to Brønsted acid sites, follow a Langmuir-Hinshelwood mechanism.

In contrast, the last reaction pathway is dictated by the Eley-Rideal mechanism where only NH₃ is adsorbed on the Brønsted acid site, followed by CH₃OH binding to the adsorbed NH₃. To obtain the desired product, methoxonium cation is first generated via the Eley-Rideal precursor complex, which then reacts with ammonia, and loses water to yield a protonated methylamine. ΔE_{sc}^{tv} related to the Eley-Rideal configuration is found to be 183.85 kJ/mol.

CONCLUSIONS

We conclude that paths II, III, IV are the suggested reaction pathways, but paths (II and IV) involving the associative mechanism are the more preferred reaction routes due to a lower activation energy as compared to the path III. The results obtained in the present study are very useful from the experimental point of view, since the adsorption and coadsorption processes on the surface site are found to play a significant role in the catalytic process.

ACKNOWLEDGEMENTS

This research was supported by the Thailand Research Fund and KURDI.

REFERENCES

- 1. I.E. Maxwell, Cattech 1, 5 (1997).
- 2. F.Haase and J. Sauer, J. Am. Chem. Soc. 117, 3780.(1995).
- 3. R.A. van Santen and G.J. Kramer, Chem. Rev. 95, 637 (1995).
- 4. A. Kogelbaner and J.A. Lercher, J. Chem. Soc. Faraday Trans. 88, 2283 (1992).
- 5. P.E. Sinclair and C.R.A. Catlow, J. Chem. Soc., Faraday Trans. 93(2), 333 (1997).
- 6. S.R. Blaszkowski and R.A. van Santen, J. Phys. Chem. 101, 2292 (1997).
- 7. J. Limtrakul, Chem. Phys. 193, 79 (1995).
- 8. J.D. Gale, Topics in Catalysis 3, 169 (1996).
- 9. J. Limtrakul and U. Ongthong, J. Mol. Struct. 435, 181 (1997).
- 10. J. Limtrakul, P. Treesakol and M. Probst, Chem. Phys. 215, 77 (1977).
- 11. J. Limtrakul and D. Tantanak, Chem. Phys. 208, 331 (1996).
- 12. J. Baker, Comput. Chem. 7, 385 (1986); 8, 563 (1987).
- 13. M.J. Frisch, G.W. Trucks, H.B. Schlegel, P.M.W. Gill, B.G.Johnson, M.W. Wong, J.B. Foresman, M.A. Robb, M. Head-Gordon, E.S. Replogle, R. Gomperts, J.L. Andres, K. Raghavachari, I.S. Binkley, C. Gonzalez, R.L. Martin, D.J. Fox, D.J. DeFrees, J. Baker, J.J.P. Stewart and J.A. Pople, Gaussian 94 (Gaussian Inc., Pittsburgh, 1994).
- 14. R. Ahlrichs, M. Bär, M. Häser, H. Horn and C. Kömel, Chem. Phys. Lett. 162, 165 (1989).
- 15. U. Messow, K. Ouitzsch, and H. Herden, Zeolites 4, 255 (1984).
- V. Gutmann, The donor-acceptor approach to molecular interactions (Plenum Press, New York, 1978).

เคมีของซีโอไลต์

จำรัส ลิ้มตระกูล

ห้องปฏิบัติการวิจัยเคมีคอมพิวเตอร์ และเคมีประยุกต์ ภาควิชาเคมี คณะวิทยาศาสตร์ มหาวิทยาลัยเกษตรศาสตร์ กรุงเทพ 10900

E mail: jumras@chem.sci.ku.ac.th; Phone: 9428034-5

ซีโอไลต์คืออะไร? มีสมบัติ อย่างไร?

ชีโอไลต์เป็นสารประกอบอะลูมิในซิ ลิเกต (1) (crystalline aluminosilicates) มี โครงสร้างเป็นรูพรุนมีโพรงและช่องว่าง ขนาดตั้งแต่ 2-10 Å (ตารางที่ 1) ซึ่งเป็น ลักษณะพิเศษเฉพาะตัวที่เด่นชัด สมบัติของ ซีโอไลต์ที่นำเอาไปใช้ประโยชน์ เช่น การแลก เปลี่ยนไอออน (ion exchange) การดูดซับ (adsorption) การดูดขับแก๊ส สารอาหาร น้ำ ตลอดจนโมเลกุลอินทรีย์ และสมบัติที่สำคัญ มากอย่างหนึ่งคือเป็นตัวเร่งปฏิกิริยา

ตารางที่ 1 คุณลักษณะของชีโอไลต์ชนิดต่าง ๆ (2)

สัญลักษณ์	ชื่อ	ขนาดของโพรง (Å)	อัตราส่วน Si/Al
FAU	Faujasite	7.4	1.25 (Zeolite X)
			2.80 (Zeolite Y)
LTL	Zeolite L	7.1	3
MOR	Modenite >	6.5 × 7.0	5
MFI	ZSM-5	5.3× 5.6	22
		5.1 × 5.5	
BEA	Zeolite Seta	7.6 × 6.4	30
•		5.5 ×5.5	

เคมีของซีโอไลต์

จำรัส ลิ้มตระกูล

ห้องปฏิบัติการวิจัยเคมีคอมพิวเตอร์ และเคมีประยุกต์

ภาควิชาเคมี คณะวิทยาศาสตร์ มหาวิทยาลัยเกษตรศาสตร์ กรุงเทพ 10900

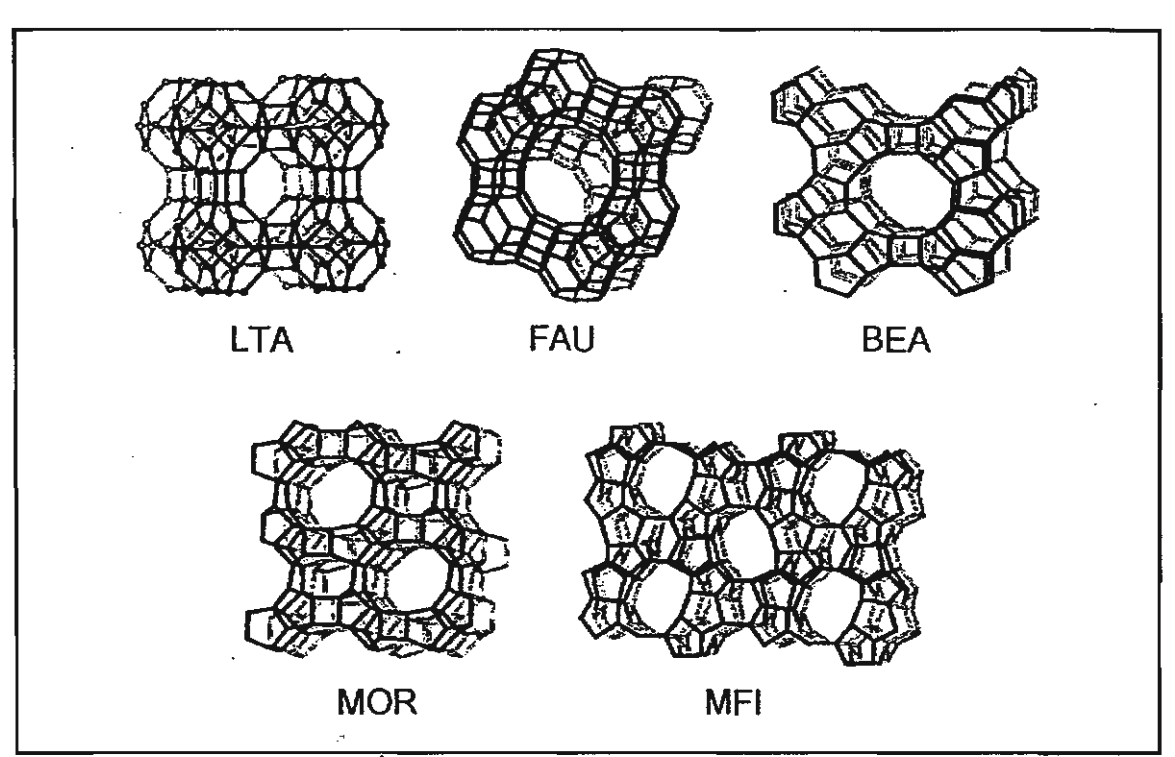
E mail: jumras@chem.sci.ku.ac.th; Phone: 9428034-5

ซีโอไลต์คืออะไร? มีสมบัติ อย่างไร?

ชีโอไลต์เป็นสารประกอบอะลูมิในชื ลิเกต (1) (crystalline aluminosilicates) มี โครงสร้างเป็นรูพรุนมีโพรงและช่องว่าง ขนาดตั้งแต่ 2-10 Å (ตารางที่ 1) ซึ่งเป็น ลักษณะพิเศษเฉพาะตัวที่เด่นชัด สมบัติของ ชีโอไลต์ที่นำเอาไปใช้ประโยชน์ เช่น การแลก เปลี่ยนไอออน (ion exchange) การดูดขับ (adsorption) การดูดขับแก๊ส สารอาหาร น้ำ ตลอดจนใมเลกุลอินทรีย์ และสมบัติที่สำคัญ มากอย่างหนึ่งคือเป็นตัวเร่งปฏิกิริยา

ตารางที่1 คุณลักษณะของซีโอไลต์ชนิดต่าง ๆ (2)

สัญลักษณ์	ชื่อ	ขนาดของโพรง (Å)	ขัตราส่วน Si/Al
FAU	Faujasite	7.4	1.25 (Zeolite X)
			2.80 (Zeolite Y)
LTL	Zeolite L	7.1	3
MOR	Modenite :	6.5 × 7.0	5
MFI	ZSM-5	5.3× 5.6	22
		5.1 × 5.5	
BEA	Zeolite Beta	7.6 × 6.4	30
		5.5 ×5.5	



รูปที่ 1 แสดงโครงสร้างซีโอไลต์ชนิดต่างๆ

ซีโอไลต์ทำอะไรได้บ้าง?

1. การแลกเปลี่ยนไอออน (ion exchange)

ในปัจจุบันนิยมใช้ชีโอไลต์เป็นส่วน
ผสมในการทำสารชักล้าง โดยจะใช้ชีโอไลต์
แทนสารฟอสเฟต (phosphates) ซึ่งเป็นตัว
water softening agents ที่อันตรายต่อสิ่ง
แวดล้อม ซีโอไลต์ (zeolite A) มีโลหะ
โชเดี ยมซึ่งสามารถแลกเปลี่ ยนกับโลหะ
แคลเซียมและแมกนีเซียมได้เป็นอย่างดีและ
ไม่เป็นอันตรายต่อสิ่งแวดล้อม

การบำบัดนำ้เสีย ซีโจไลต์สามารถ ขจัด แอมโมเนียจากนำ้เสีย โดยการแลก เปลี่ยนแอมโมเนียมแคตใจจจนกับโลหะ โซเดียมที่อยู่ในโพรงซีโอไลต์ได้เป็นอย่างดี ดังนั้นซีโอไลต์ที่สังเคราะห์ขึ้นสามารถบำบัด นำ เสียได้ เป็นอย่างดี นอกจากนั้นยัง สามารถใช้ ขจัดไอโซโทปกัมมันตรังสี (cesium and strontium radioisotopes) จากกากนิวเคลียร์ (nuclear wastes)

2. การดูดซับ (adsorption)

มีการใช้ชีโอไลต์เป็นตัวดูดชับสาร ต่าง ๆ รวมทั้งการประยุกต์ใช้ในกระบวนการ ทำให้แห้ง (drying) กระบวนการทำให้ บริสุทธิ์ (purification) และ กระบวนการ แยกสาร (separation)

3. การเร่งปฏิกิริยา (catalysis)

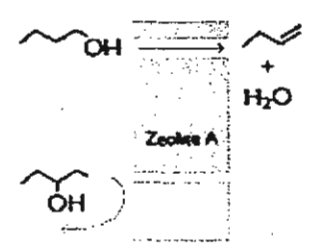
นักเคมีทำการสังเคราะห์สารที่มี
โครงสร้างคล้ายชีโอไลต์ และเรียกสารกลุ่มนี้
ว่า molecular sieves จากการสังเคราะห์
และออกแบบโครงสร้างจึงทำให้สารดังกล่าว
มีคุณค่าและ คุณประโยชน์ที่สำคัญใน
อุตสาหกรรมปิโตรเคมี เช่น ใช้เป็นตัวเร่ง
ปฏิกิริยาในกระบวนการเปลี่ยนแปลงเมธา
นอลเป็นไฮโดรคาร์บอน (methanol to
olefin) และ การแตกตัวด้วยตัวเร่งปฏิกิริยา
(catalytic cracking) เป็นต้น

ชีโอไลต์มีสมบัติเป็นกรด (Br nsted acid sites) และมีโครงสร้างเป็นภูพรุน และ เป็นโพรง ทำให้มีสมบัติโดดเด่น เช่น มี ความสามารถในการเลือกเกิดปฏิกิริยาตาม ภูปทรง (shape selectivity) ซึ่งอาจแบ่งได้ เป็น 3 แบบ ได้แก่ การเลือกเกิดปฏิกิริยาตามภูปทรงของสารตั้งต้น (reactant shape selectivity) การเลือกเกิดปฏิกิริยาตามภูปทรงของสารผลิตภัณฑ์ (product shape selectivity) และการเลือกเกิดปฏิกิริยาตาม ภูปทรงของสถานะแทรนซิชัน (transition state shape selectivity)

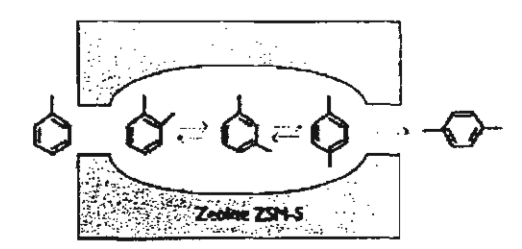
การเลือกเกิดปฏิกิริยาตามรูปทรง ของสารตั้งต้น (reactant shape selectivity) ชีโอไลต์เอสามารถเร่งปฏิกิริยาสูญเสียน้ำ (dehydration) ของ 1-butanol ได้อย่างดี แต่ ไม่ทำปฏิกิริยากับ 3-pentanol ซึ่งมีขนาด ใหญ่กว่า (ดูรูปที่ 2.1)

การเลือกเกิดปฏิกิริยาตามรูปทรง
ของสารผลิตภัณฑ์ (product shape
selectivity) ปฏิกิริยาเมธิลเลขัน
(methylation) ของโทลูอีนซึ่งเกิดขึ้นภายใน
โพรงของซีโอไลต์ ZSM5 จะเกิดขึ้นที่
ตำแหน่งพารา (para) เพื่อเกิดเป็นพาราไซลี
น (p-xylene) ซึ่งมีขนาดเล็กกว่าสาร
ผลิตภัณฑ์ชนิดอื่นๆ (คูรูปที่ 2.2)

การเลือกเกิดปฏิกิริยาตามรูปทรงของสถานะแทรนซิขัน (transition-state selectivity) ปฏิกิริยาการเกิดวงแหวน (cyclization) ของ 2,4-pentadiene สามารถเกิดขึ้นภายในโพรงของซีโอไลต์ mordenite แต่ไม่สามารถเกิดขึ้นภายในโพรงของซีโอ ไลต์ ZSM5 ซึ่งมีขนาดของโพรงเล็กกว่า สถานะแทรนซิขัน (คูรูปที่ 2.3)



2.1 การเลือกเกิดปฏิกิริยาตามรูปทรงของสารตั้งต้น (reactant shape selectivity)



2.2 การเลือกเกิดปฏิกิริยาตามรูปทรงของสารผลิตภัณฑ์ (product shape selectivity)



2.3 การเลือกเกิดปฏิกิริยาตามรูปทรงของสถานะแทรนซิขัน (transition-state selectivity) รูปที่ 2 แสดงลักษณะการเลือกเกิดปฏิกิริยาตามรูปทรงของสารตั้งต้น, สารผลิตภัณฑ์ และ สถานะแทรบซิชับ

งานวิจัยเกี่ยวกับซีโอไลต์

ชีโอไลต์มีมากกว่า 600 ชนิด (2538) แต่พอจะแบ่งกลุ่มตามชนิดของโครงสร้าง ได้ ประมาณ 40 ชนิด องค์ประกอบหลักที่ทำให้ ชีโอไลต์มีสมบัติแตกต่างกันคือ อัตราส่วน ของ ชิลิกอน และ อะลูมิเนียม การเปลี่ยน อัตราส่วนดังกล่าวมีผลก่อให้เกิดการเปลี่ยน แปลงกัมมันตภาพเชิงเร่งปฏิกิริยา (catalytic activity) และความเสถียรของ โครงสร้างชีโอ ไลต์

การแทนที่ธาตุ Si และ Al ด้วยธาตุ อื่น เช่น Ga, Ge, P, B และ Fe ในโครงสร้าง ชีโอไลต์ ทำให้ เกิด acidic bridging hydroxyl (≡AIOH-Ga≡, ≡Si-OH-Ga≡, ≡Si-OH-B≡) ซึ่งก่อให้เกิดการเปลี่ยนแปลง สภาพมีขั้ว (polarity) และความเป็นกรดของ ชีโอไลต์

การศึกษาและวิจัยถึงความสัมพันธ์
ของโครงสร้างและกับมันตภาพเชิงเร่ง
ปฏิกิริยาทำให้เราสามารถออกแบบและ
สังเคราะห์ซีโอไลต์ที่มีสมบัติใหม่ๆ เพื่อน้ำมา
ใช้ในปฏิกิริยาเคมีต่างๆ ได้ตามต้องการ และ
ขณะนี้ได้มีการศึกษาและวิจัยเกี่ยวกับซีโอ
ไลต์เมมเบรน (zeolite membrane) เพื่อใช้
ในการแยกสารประกอบไฮโดรคาร์บอน (3)
นอกจากนี้ได้มีการสังเคราะห์ transitionmetal oxide cluster ขึ้นภายในโพรงของซีโอ
ไลต์เพื่อนำมาใช้ในปฏิกิริยาออกซิเดชันของ
สารประกอบไฮโดรคาร์บอน (4)

กลุ่มเคมีชีโอไลต์และวิศวกรรมตัวเร่ง ของภาควิ ชาเคมี และวิ ศวกรรมเคมี มหาวิทยาลัยเกษตรศาสตร์ ได้ศึกษาและวิจัย ในหัวข้อต่อไปนี้ (5-14)

- Adsorption and coadsorption in zeolite
- Molecular aspects of heterogeneous catalysis
- Surface reaction dynamics in zeolitic catalysts
- Catalytic cracking (reaction & mechanism)
- Development of new and/or better catalytic reaction pathways via the explorative computational methods and the synthesis of new catalytic materials
- Other areas of developing use of zeolite like environmental chemistry

กิตติกรรมประกาศ

ขอขอบคุณสำนักงานกองทุนสนับ สนุนการวิจัยและสถาบันวิจัยและพัฒนา แห่งมหาวิทยาลัยเกษตรศาสตร์

เคกสารค้างคิง

- 1. Dyer, A. (1988). An introduction to zeolite molecular sieves. John Willey & Sons, New York.
- 2. Ono, Y. (1997). Solid acids and bases catalyze selective alkylations. Cattech.1, 31-38.
- 3. Gavalas, G.R., Yan, Y. and Davis, M.E. (1997). Preparation of selective zeolite ZSM-5 by a postsynthetic coking treatment, J. Membr. Sci.123, 95.
- 4. Pantu, P. (1997). Private communication.
- 5. Limtrakul, J. and Treesukol, P. (1997). Structures and potential energy hypersurface of faujasitic catalysts. Chem. Phys. 215, 77-87.
- 6. Limtrakul, J. and Tantanak, D. (1996). Cationic, structural, and compositional effects on the surface structure of zeolitic aluminosilicate catalysts. J.Chem.Phys. 208, 331-340.
- 7. Limtrakul, J. (1995). Adsorption of methanol in zeolite catalysts. Chem.Phys.193, 79-87.

- Limtrakul, J. and Tantanak, D. (1995).
 Structures, energetics and vibrational frequencies of zeolitic catalysts: a comparision between density functional and post-Hatree-Fock approaches. J. Mol. Struct. 358, 179-193.
- Limtrakul, J. and Yoinuan, J. (1994).
 Formation of ammonium cation at the Brønsted site in SAPO catalysts.
 Chem. Phys. 184, 51-57.
- 10.Limtrakul, J., Yoinuan, J. and Tantanak, D. (1994). Adsorption complexes of ammonia on germanium- and gallium-modified zeolites. J. Mol. Struct. 312, 183-194.
- 11.Limtrakul, J. (1993). Molecular modelling and catalytic properties of

- materials. *J. Mol. Struct.* 288, 105-110.
- 12.Limtrakul, J. and Hannongbua-Polman, S. (1993). Catalytic properties of a free hydroxyl on a silica, a zeolite, and modified zeolites: quantum-chemical model calculations. J. Mol. Struct. 280, 139-145.
- 13.Chareonpanich, M. et. al (1994).
 Selective production of BTX by hydrocracking of coal over zeolite catalyst. Energy Fuels 8, 1522.
- 14.Chareonpanich, M. et. al (1996).
 Hydrocraccking of aromatic hydrocarbon over USY- zeolite.
 Energy Fuels 10, 927.

ผลงาน

ผลงานที่ตีพิมพ์และกิจกรรมอื่น ๆ ที่เกี่ยวข้อง

- Limtrakul, J. and Tantanak D, J. Molecular Structure, 358 (1996) 179-193
 "Structures, energetics, vibrational frequies of zeolitic of zeolitic catalyst, a comparison with density functional and post Hartree-Fock",
- Limtrakul, J. and Tantanak, J. Chemical Physics, 208 (1996) 331-340.
 "Cationic, structure, and composition effects on the surface structure of zeolitic aluminosilicate catalysts".
- Limtrakul, J. and Treesukol P, J. Chemical Physics, 215 (1997) 77-87.
 "Structures and potential energy surface of faujasitic zeolite / water"
- Limtrakul J. and Onthong U. J Molecular Structure 435 (1998) 181-192.
 "Coadsorption of ammonia and methanol on H-zeolites and alkaline-exchanged zeolites
- Limtrakul J. "Structure and Reaction Pathways in Zeolitic Systems" in Zeolite Chemistry and Catalysis , M.M.J. Treacy, B. Marcus, J.B. Higgins and M. E. Bisher (Eds.) Materials Research Society, USA.

ผลงานอื่นๆ และรางวัลที่ได้รับ 2538-2541

- นักวิจัยที่มีผลงานดีเยี่ยมของเมธีวิจัย สกว. ประจำปี 2539
- นักวิจัยที่มีผลงานดีเยี่ยมของเมธีวิจัย สกว. ประจำปี 2540
- รางวัลผลงานวิจัยดีเด่นทางเคมีในรูปโปสเตอร์ในการประชุมวิทยาศาสตร์และเทคโนลียีแห่ง ประเทศไทย ครั้งที่ 22 ประจำปี 2539
- รางวัลผลงานวิจัยดีเด่นทางเคมีในการประชุมวิทยาศาสตร์และเทคโนลียีแห่งประเทศไทย ครั้งที่
 23 ประจำปี 2540
- รางวัลนักวิจัยดีเด่นแห่งชาติสาขาเคมี และเภสัช ประจำปี 2541 จากสภาวิจัยแห่งชาติ
- บุคลากรผู้มีผลงานดีเด่นทางวิชาการ มหาวิทยาลัยเกษตรศาสตร์ ประจำปีการศึกษา 2541
- ผลงานวิจัยดีเด่นสาขาวิทยาศาสตร์และเทคโนลียี "ครบรอบยีสิบงานวิจัย มก. สถาบันวิจัย มก.

จำนวนและรายละเอียดที่ได้รับเชิญเป็นวิทยากร

- Structure and reaction pathways in Zeolites, 12th International Zeolite Conference, 1998
 Baltimore, MD. USA.
- The role of molecular modelling in chemistry, สมาคมเคมี ห้องประชุมใหญ่ มหาวิทยาลัย เกษตรศาสตร์ กรุงเทพมหานคร
- ศักยภาพของนักวิทยาศาสตร์ไทย องค์ปาฐก "ปาฐกถาศาสตราจารย์ ดร.แถบ นีละนิธิ" 23 สิงหาคม 2541 ณ ห้องราชเทวี 2 โรงแรมเอเชีย กรุงเทพมหานคร
- Chemistry 1998 and Beyond การประชุมวิชาการวิทยาศาสตร์และเทคโนโลยีแห่งประเทศไทย ครั้งที่
 24 19-21 ตุลาคม 2541 ศูนย์ประชุมสิริกิติ์ กรุงเทพมหานคร
- Structure and Reactivity in Zeolites กรมวิทยาศาสตร์บริการ กระทรวงวิทยาศาสตร์เทคโนโลยีและ สิ่งแวดล้อม กรุงเทพมหานคร
- Catalyst Design 11 กันยายน 2541 คณะวิทยาศาสตร์ มหาวิทยาลัยเกษตรศาสตร์ กรุงเทพมหานคร
- หลักสูตร วท.บ.เคมี แนวใหม่ มหาวิทยาลัยทักษิณ สงขลา
- บรรณาธิการวารสาร KU Science Journal

การเชื่อมโยงทางวิชาการกับนักวิชาการอื่น ๆทั้งในและนอกประเทศ

- Chemical Engineering Department, Kasetsart University. In close collaboration with Chemical Engineering Department at Washington University, USA.
 Industrial applications of zeolite catalysis.
- Chemistry Department, University of Utah, Utah, USA.
 Development and Exploration of embedded Cluster Approach and Direct Dynamics for heterogeneous catalysis
- Laboratory for Molecular Spectroscopy, Bordeaux University, France.
 Surface Characterization of Advanced Materials
- Institutes of Inorganic and Theoretical Chemistry, University of Innsbruck and University of Vienna.
 - Computer Simulations of Surface Physical Chemistry and Drug Design.
- Molecular Simulations Inc., Sydney, Australia.
 Computer Aided Materials and Drug Design.
- Institute of Physical Chemistry & Electrochemistry, University of Karlsruhe, Germany.
 Development and Exploration of Computational chemistry codes.

Computer Simulations of Surface Physical Chemistry and Drug Design.

- Molecular Simulations Inc., Sydney, Australia.
 Computer Aided Materials and Drug Design.
- Institute of Physical Chemistry & Electrochemistry, University of Karlsruhe, Germany.

Development and Exploration of Computational chemistry codes.

ภาคผนวก

The Surface Structure and Catalytic Properties of Zeolite and Molecular Sieve Catalysts

Pl: Jumras Limtrakul

Chemistry Department, Faculty of Science, Kasetsart University

Executive Summary

Rational catalyst design, notably zeolites and molecular sieves, represents one of the most rewarding challenges in catalysis research. Zeolites possess three dimensional microporous crystalline solid. Their catalytically active acid-sites within the complex porous framework structure provide unique properties that make them very attractive industrial materials. They play a significant role in chemicals and fuels production worth over \$1000 billion per year. Zeolites and molecular sieves can be tailored or chosen to maximize the product of target molecules by employing state-of-the-art techniques. Our aim is to develop strategies for tailoring the structural and chemical properties of catalyst materials and to explore the potential of new catalytic materials.

 Structures, energetics and vibrational frequencies of zeolitic catalysts: a comparison between density functional and post-Hartree-Fock approaches Limtrakul, J. and Tantanak D, J. Molecular Structure, 358 (1996) 179-193.

We have carried out LSD and NLSD functional methods with 3-21G, 6-31G*, 6-311G* and DZVP basis sets to investigate the structures, energetics and vibrational frequencies for silanol, disiloxane, and different zeolite clusters. Some smaller models have also been calculated at the MP2 level. The individual geometrical parameters calculated at the BLYP and VWN levels with a modestly sized basis sets (6-311G*) generally yield good results compared to MP2 with much less computational effort. Comparing BLYP and VWN results with MP2, the former has a significant lengthening effect on the weaker A-O bond which does not occur with the latter. The Si-O(H)-Al and Si-O-H bond angles of zeolites are not appreciably affected by the inclusion of NLSD. However, the NLSD was found to be important for a better description of the floppy Si-O-

Si bond angle for disiloxane. The proton affinity of H3SiOHAlH3, a widely employed model of a Brønsted acid site in zeolites, is virtually identical to that of MP2/DZP and is also close to the result from G1 theory within the desired 10 kJ mol-1 accuracy. For this cluster model, the BLYP VOH value is calculated to within 130 cm-1 of the experimental value. We expect that the same accuracy from the BLYP/6-311G* procedure will be applied to larger zeolite clusters in the future.

Structures and potential energy surface of Faujasitic zeolite/water
 Limtrakul, J. and Treesukol, P., Chemical Physics, 215 (1997) 77-87.

We have presented a density functional study of faujasitic zeolites and their complexes with water using the B3LYP functionals and the basis sets 6-31G(d), 6-31G(d,p), 6-311G(d), 6-311G (d,p) and 6-311+G(d,p). The agreement between DFT/B3LYP-6-311+G(d,p) proton affinities and the corresponding CPF and G1 values are excellent. Comparing the older BLYP and VWN functionals, with the recently introduced B3LYP functionals, the latter yields superior accuracy. This artificial significant lengthening effect on the weaker Al-O bond in the BLYP and VWN calculations does not occur with B3LYP. The Si-O(H)-Al and Si-O-H bond angles of zeolites do not appreciably depend on the inclusion of non-local effects in the density functional. The 6-31G (d) basis set in DFT prediction of the faujasitic structure yields good results and is an economic choice for large systems. The predicted PA of the faujasitic catalyst is estimated to be 294±3 kcal/mol, which is in the range of experimentally determined value of 291-300 kcal/mol. The faujasite catalyst/water structure is stabilized at the bridging O-H group by two H-bonds with binding energy of -20.3 kcal/mol. Comparison with hydrogen halides and related complexes of water demonstrates that the faujasite is a strong acid. An analytical potential for the interaction to faujasitic zeolite with water was derived by fitting the ab initio interaction energies which we plan to employ in simulations studies of petrochemical catalyst/water systems.

Coadsorption of ammonia and methanol on H-zeolites and alkaline-exchanged zeolites
 Limtrakul J. and Onthong U. J. Molecular Structure 435 (1998) 181-192.

We have carried out HF and B3LYP methods with 6-31G* basis set to investigate the coadsorption of methanol and ammonia on H-zeolites (H-Z) and alkaline-exchanged zeolites (Na-Z). Comparing HF and B3LYP results with available experimental data, the B3LYP yields structural parameters which are in good agreement with experimental data. The Al...H distance of zeolite has been estimated experimentally as 238±4 pm, where as our B3LYP value is 239.7

pm. A comprehensive study of the coadsorption of absorbate molecules with the surface hydroxyl reveals several interesting points. Structure Na-Z/[CH3OH][NH3] is lower in energy than Na-Z/[NH3] [CH3OH], which suggests that the former is more favourable in the coadsorption process. The reaction mechanism of coadsorption of methanol and ammonia on H-Z is that the ammonia is found to stabilize to the BrØnsted acid site of H-Z, generating an ammonium cation, which acts as an active site for methanol.

 Cationic, structural, and compositional effects on the surface structure of zeolitic aluminosilicate catalysts

Limtrakul, J. and Tantanak, J. Chemical Physics, 208 (1996) 331-340.

The cationic, structural and compositional effects on the structure and bonding of different types of \equiv Si-OH-Al \equiv units in the secondary building unit of zeolite cluster models (OH)8HyAlxSi8-xO12)(x-y)- (x, y=0, 1, 2, 4) and the silica model (OH)8Si8O12 have been investigated with the DFT method. Full optimization of all mentioned structural isomer clusters have been carried out at VWN/6-31G* and BLYP/6-31G*. All isomers of the double four-membered ring aluminosilicate (D4R) demonstrate that Dempsey's rule may be violated in this type of zeolite. The well-known Loewenstein's \equiv Al-O-Al \equiv avoidance rule has been once again confirmed by us. The results of D4R with varying Si/Al ratio indicate that the higher the ratio, the lesser the proton is restricted which results in a higher acidic strength. The cations, H+ and Li+, are found to have a profound effect on the important structural parameters (Si-O, Al-O, O-H bonds and SiOHAl angle) of D4R. The marked difference between the cations is that the H+ is singly bonded while the Li+ is doubly bonded to the framework. This excellent results indicate that the catalytic activity of zeolites is also enhanced by the presence of cations, in addition to a compositional effect.